Advanced Devices & Instrumentation
A SCIENCE PARTNER JOURNAL

REVIEW ARTICLE

Spin-Related Superconducting Devices for Logic and Memory Applications

Yu He[1†], Jiaxu Li[1†], Qiusha Wang[1], Hisakazu Matsuki[2], and Guang Yang[1*]

[1]Fert Beijing Institute, MIIT Key Laboratory of Spintronics, School of Integrated Circuit Science and Engineering, Beihang University, Beijing 100191, China. [2]Department of Materials Science & Metallurgy, University of Cambridge, 27 Charles Babbage Road, Cambridge CB3 0FS, UK.

*Address correspondence to: gy251@buaa.edu.cn
†These authors contributed equally to this work.

Citation: He Y, Li J, Wang Q, Matsuki H, Yang G. Spin-Related Superconducting Devices for Logic and Memory Applications. *Adv. Devices Instrum.* 2023;4:Article 0035. https://doi.org/10.34133/adi.0035

Submitted 6 July 2023
Accepted 7 November 2023
Published 8 December 2023

Recently, there has been a surge of research in the field of superconducting spintronics, which combines superconductivity and magnetism. This emerging field is considered an alternative or complementary approach to traditional complementary metal-oxide semiconductor (CMOS) technology, offering high efficiency and effectiveness. Furthermore, the unique physical phenomena resulting from the interplay of these two competing properties have attracted increasing attention for their potential application in low-power quantum computing. In this review, we focus on the latest advancements in spin-related superconducting logic devices, specifically categorized as superconducting diodes based on their semiconductor counterparts. Additionally, given the ultralow operating temperatures required for these devices, we provide a comprehensive overview of compatible cryogenic memory technologies that incorporate spin-related principles. Finally, we address the key challenges currently hindering the practical implementation of spin-related superconducting electronics and offer insights and directions for future research in this field.

Introduction

In recent years, there has been significant excitement and attention surrounding the emergence and advancement of large language models (LLMs), such as Claude, GPT-4, PanGu-Σ, and others. These models, which utilize artificial intelligence generated content (AIGC), are regarded as a result of combining big data with enhanced computational power. Consequently, power efficiency has become a critical performance indicator at the server end, in addition to user-end accuracy. However, at the circuit and architecture level, the miniaturization of electronic computing devices presents challenges in terms of power consumption and heat dissipation. These challenges increasingly hinder the development of reliable and controllable high-density very large scale integration (VLSI) circuits. As electronic component sizes continue to shrink toward their physical limits, quantum mechanisms gradually take precedence, rendering Moore's law obsolete. This shift has prompted the exploration of alternative electronic devices with novel physical phenomena, which hold promise for overcoming these physical limitations and advancing energy-efficient high-performance computing.

Spintronics, using the degree of freedom of spin apart from the electron charge, offers a new set of methods for data processing from novel computational paradigms [1] to next-generation hybrid devices [2]. Spin-related hybrid spintronic devices facilitate the development of high-speed and low-power computing systems, but Joule heat still exists in such devices where both spin and charge coexist [3,4]. Spin transfer torque magnetic random access memory (STT-MRAM), for example, has no standby power consumption compared to its conventional counterpart like dynamic random access memory (DRAM), but the process of writing using spin-polarized current still requires a high density current (usually of the order of 10^{11} A/m^2), thus generating a thermal gradient in memory devices and unavoidable Ohmic losses [4]. The study of the interaction between spin, electricity, and heat, a frontier intercrossed research area called spin caloritronics, has indeed offered possible solutions to utilize such thermal gradient to reduce power dissipation [5,6]. From the perspective of logic device applications, despite efforts in developing beyond von Neumann architecture in which logic and memory are intimately combined in nonvolatile memory components [7], however, there is scarcely any viable transistor-like device based on processing spin signal information similar to their semiconductor counterparts [8,9].

Superconducting spintronics takes one step further while narrowing the scope of research to novel physical phenomena by combining superconducting phase coherence and magnetism [4,10]. Usually, the two competing properties hardly coexist in one material, due to the strong destructiveness of ferromagnetism on conventional superconductivity. The spin-singlet Cooper pairs ($|\uparrow\rangle|\downarrow\rangle - |\downarrow\rangle|\uparrow\rangle$) induced by electron–phonon interaction, which are considered as charge flow carriers in conventional s-wave superconductors, will experience pair breaking in the presence of a strong magnetic field according to Ginzburg's theory [11]. Therefore, the proximity effect between a superconductor thin film and a ferromagnet

leads to the suppression of superconductivity, specifically the critical temperature T_c and the Josephson critical current I_c. However, advances in micro-/nanofabrication technologies have enabled researchers to manipulate the thickness of thin films with precision, allowing for the analysis of intriguing physical phenomena that emerge at interfaces between s-wave superconductors and ferromagnets (SC/FM) [10,12–14]. Pair correlations that leak from the superconductor to the ferromagnet rapidly decay in a distance-dependent oscillatory way within the thickness range, or the superconducting coherence length ξ_s [15,16]

$$\xi_s = \sqrt{\frac{\hbar D_F}{E_{E_X}}}, \quad (1)$$

where the diffusion constant $D_F = v_F l_e/3$ in the ferromagnet is related to the mean free path of the electron l_e and the Fermi velocity v_F. The ferromagnetic exchange energy E_{EX} can be approximated by $E_{EX} \approx k_B T_C$, where T_C is the Curie temperature. In the presence of a magnetically inhomogeneous SC/FM interfaces, such as an orthogonal magnetic exchange field, the conversion of spin-singlet Cooper pairs ($|\uparrow\downarrow\rangle - |\downarrow\uparrow\rangle$) into spin-triplet Cooper pairs ($|\uparrow\uparrow\rangle$, $|\downarrow\downarrow\rangle$, or $|\uparrow\downarrow\rangle + |\downarrow\uparrow\rangle$) occurs, which can be explained by a combination of spin-mixing and spin-rotation processes [12,17]. Compared to spin-singlet pairs, symmetric spin-triplet pairs, ($|\uparrow\uparrow\rangle$ and $|\downarrow\downarrow\rangle$), are hardly influenced by the pair-breaking effect induced by the Zeeman field, thus being recognized as long-range triplet components (LRTCs). Such LRTCs are first reported to be hundreds of nanometers even in half metallic CrO_2 (110) single crystal thin film [18] (much longer than the coherence length of conventional s-wave superconductors). From the application point of view, in conventional spintronics, the phenomenon of spin-tansfer torque provides a new way to manipulate the magnetization of magnetic nanostructures by a spin-polarized current [7], but in s-wave superconductors, the spin-singlet pairs with zero spin angular momentum are unable to carry spin-polarized current in spite of dissipationless charge current. The novel transport phenomena at the SC/FM interface, nevertheless, facilitated by spin-triplet Cooper pairs with both electron spins aligned in the same direction, may carry both dissipationless charge current and spin-polarized current, thus envisioning a promising pathway to supplement traditional spintronics by alleviating unavoidable Ohmic losses.

Therefore, both the superconducting and hybrid superconducting spintronic computing paradigms are believed to be able to overcome conventional technology due to their competitiveness in power and energy efficiency. In addition to the design of spin-related logic and memory devies, which will be discussed below, however, the most critical features really setting them aside from being widely applied are the cryogenic cooling requirements, from installing suitable cryocoolers to compensating noises from vibration to electromagnetic interference (EMI), etc., as is shown in Fig. 1 [19–21]. There is still much work regarding design improvements of the cryogenic working environment in terms of power efficiency, cost, and reliability [19]. Fortunately, in some specific cases, such as high-performance cloud computing centers, data centers, or special quantum computing systems, the whole system can be maintained at ultralow temperature, which is suitable for adopting superconducting technology to further balance and maximize system performance, or computation throughput within system power budgets [20,21]. Given the abovementioned physical and

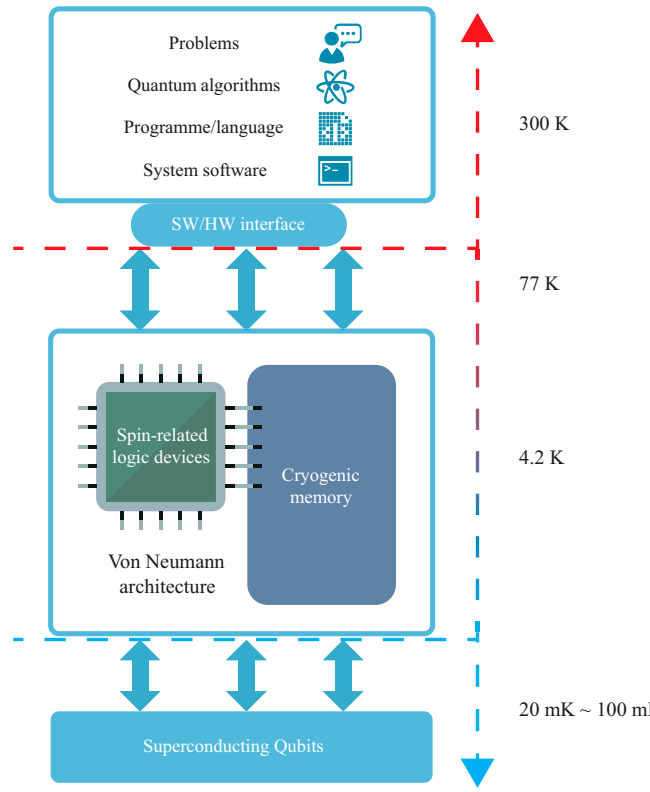

Fig. 1. Schematic illustration of the superconducting computation system within von Neumann architecture framework. Each component of the system is supposed to be maintained at different working temperatures, from 20 mK to RT, according to the actual application scenarios. The most important computing components, namely, spin-related superconducting logic and memory, should be implemented at approximately 4.2 K.

technological prospects, this review is organized around two main components in a superconducting computation system, namely, spin-related logic and cryogenic memory, and then an outlook on possible directions is highlighted for future research.

Energy-Efficient Superconducting Devices

The key inferiority that currently restricts the application of traditional spintronic devices is the high-density current required to switch magnetic states and the large amount of Joule heat. Therefore, compared to traditional semiconductor technology, the introduction of spintronic technology has little improvement in the overall energy consumption of VLSI circuits. Superconducting digital technologies, rapid single-flux quantum (RSFQ) as an example, offer a significant improvement in energy efficiency over conventional complementary metal-oxide semiconductor (CMOS) circuits and are therefore under consideration for power-efficient, high-performance computing systems (HPCs) for many years. However, such computing systems require a compatible cryogenic memory solution that has not yet been achieved. By intertwining superconductivity and magnetism, novel physical phenomena can therefore emerge and offer new sets of alternative schemes in the design of next-generation spin-related electronic components used in computation, communication, and sensing [10,22,23]. In this section, we conclude an essential overview

of the emergence and most updated progress of spin-related superconducting diodes.

Superconducting diode effect and its underlying mechanisms

Similarly to the conventional diode effect, which serve as the main building blocks for various electronic devices, e.g., rectifiers, alternating direct (AD) current converters, and photoelectric detectors, the superconducting counterparts envision many novel applications in dissipationless supercurrent logic devices. The superconducting diode effect (SDE) is a typical example of nonreciprocal superconductivity, and this direction-selective propagation of the unequal supercurrents, usually with the superconducting state in one direction, while the normal conducting state in the other, as shown in Fig. 2A, is associated with the breaking of the spatial-inversion and/or time-reversal symmetries [24–27]. For homogeneous devices or noncentrosymmetric superconducting structures, the inversion symmetry $\hat{I}$ is broken, but it does not necessarily guarantee the direction-dependent resistance [26]. Beyond broken $\hat{I}$, such sophisticated nonreciprocal responses are theoretically analyzed and categorized into four main categories depending on

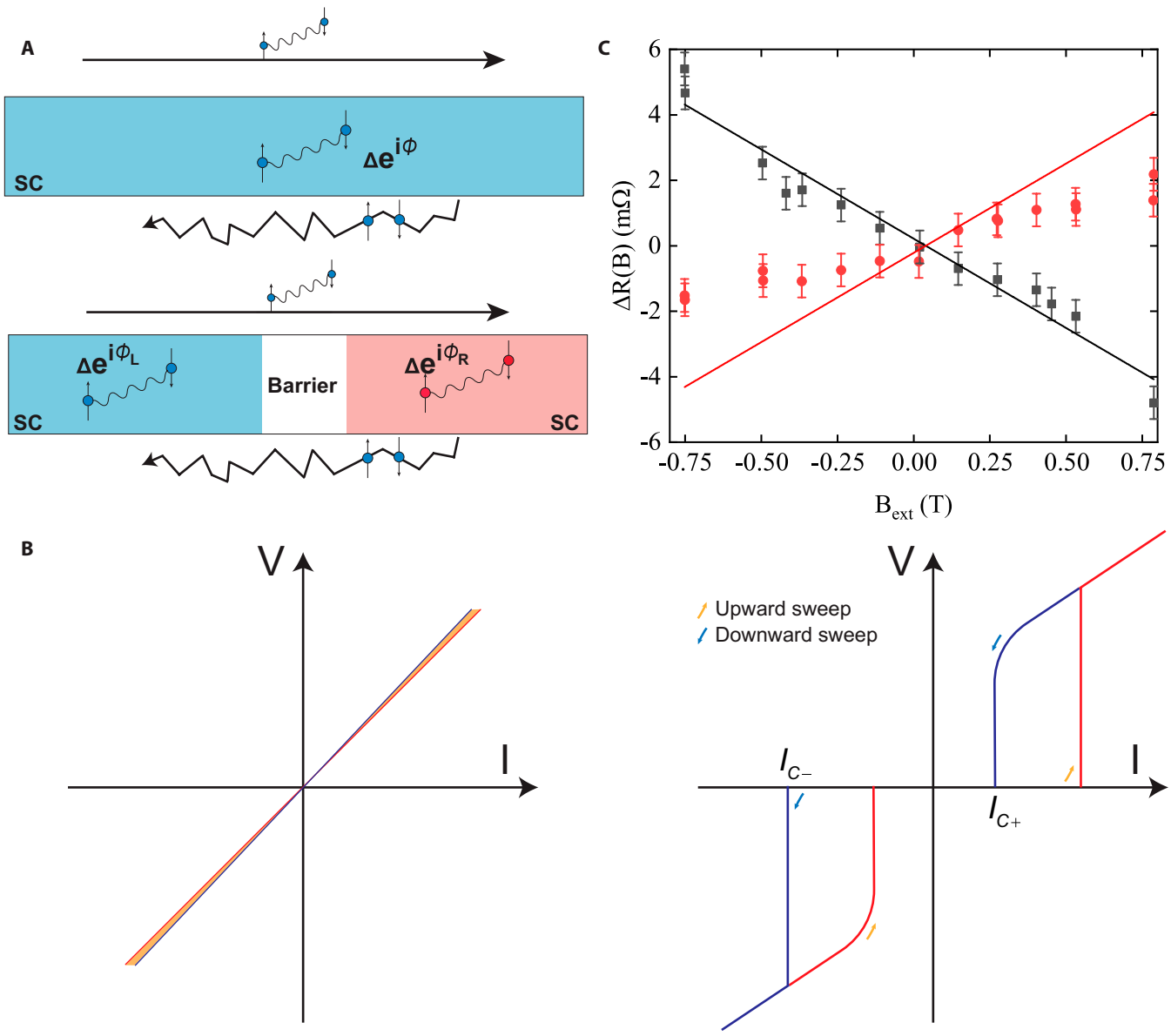

Fig. 2. (A) For diode effect in noncentrosymmetric superconducting structures such as superconductors and Josephson junctions, the superconducting state can be described by complex order parameters $\Delta e^{i\phi}$. The phase difference ϕ is then believed to cause orientation-dependent supercurrent, with normal state in one direction and superconducting in the other [122]. (B) In normal state, the nonreciprocal behavior of supercurrent is usually small, while in the superconducting fluctuation regime, such nonreciprocity is greatly enhanced below the critical current I_c. Both insets describe the nonreciprocal behavior in the asymmetric potential. It is worth mentioning that such an enhancement in nonreciprocity below critical current is attributed to the existence and coherence of Cooper pairs [28]. (C) Two-terminal MCA $\Delta R(I, B_{ext}) \equiv R(I, B_{ext}) - R(-I, B_{ext})$ of opposite flow direction (denoted by squares and triangles) as a function of the external field B_{ext}. The solid lines in the plot represent the predictions derived from Eq. 2, with the inclusion of an arbitrary vertical offset to accommodate minor asymmetries in contact resistances and electronics. It can be clearly shown that the sign of resistance difference $\Delta R(I, B_{exti})$ changed at a fixed external field B_{exti} due to the opposite current flow direction [24].

(i) the linear and nonlinear response, and (ii) $\widehat{T}$-broken and $\widehat{T}$-unbroken owing to the underlying issues, such as symmetries, quantum geometrical nature of electrons, and electron correlation [26]. Although the nonreciprocal nonlinear response can be realized by the shift current (a typical example, but not limited to, without $\widehat{T}$-symmetry breaking [26]) in noncentrosymmetric materials, experimental observations so far have only confirmed that both inversion symmetry and time-reversal symmetry are supposed to be broken to obtain such a nonreciprocal response in the fluctuation regime of noncentrosymmetric superconductors. That is to say, the breaking of inversion symmetry splits the spin bands with the spin-momentum locking in the presence of relativistic spin–orbit interaction (SOI), while time-reversal symmetry is related to the energy dispersion at different crystal momentum $\pm\boldsymbol{k}$, hence reversing the spin direction and leading to the coherence of Cooper pairs (see Fig. 2A) [28]. Therefore, in this review of spin-related superconducting devices, we mainly focus on noncentrosymmetric and time-reversal asymmetric systems.

By extending the Onsager reciprocal theorem to the superconducting fluctuation regime of resistive transition, Rikken et al. proposed a nonlinear current-dependent resistance $R(\boldsymbol{I})$ as

$$R(I) = R_0\left[1 + \beta B^2 + \gamma(\boldsymbol{B}\times\boldsymbol{z})\cdot\boldsymbol{I}\right], \tag{2}$$

where the resistance response is related to the magnetic field $\boldsymbol{B}$ and the electric current $\boldsymbol{I}$, for example, under the broken symmetry along $\boldsymbol{z}$ axis [24,25]. The parameter β describes the normal magnetoresistance, while the higher even orders in $\boldsymbol{B}$ that are also allowed in all conductors are neglected. The finite coefficient γ, or magnetochiral anisotropy (MCA), quantifies the strength of this nonreciprocity and gives rise to different resistance $R(\pm I)$ according to the relative direction of transport of electric current shown in Fig. 2B, typically with only one of $R(\pm I)$ showing zero resistance behavior in the superconducting cases. The finite MCA coefficient in the linear magnetic field-dependent term, which is the third term on the right side of Eq. 2, is typically small in normal conductors (typically of the order of around 10^{-3} to $10^{-2}\ \mathrm{T^{-1}A^{-1}}$). This is because the SOI energy (E_{SOI}) and the magnetic energy ($\mu_B B$) are relatively small compared to the Fermi energy (E_{EF}) by five orders of magnitude. Therefore, they cause weak perturbations $(\mu_B B/\varepsilon_F)(\lambda/\varepsilon_F)$. However, in the superconducting phase, the coefficient γ becomes significantly large, denoted as $\gamma = \gamma_S$. This occurs when comparing the SOI energy E_{SOI} to the superconducting gap (Δ_{SC}), i.e., (ε_F/Δ). It can also be inferred from the third term on the right side of Eq. 2 that the applied $\boldsymbol{B}$, $\boldsymbol{I}$ and the direction of broken symmetry should be orthogonal to each other to achieve such symmetry condition. Recent experimental work has further confirmed such a large MCA coefficient and related nonreciprocal transport phenomena when approaching the superconducting transition temperature T_c in MoS_2 [28], $SrTiO_3$ [29], $NbSe_2$ [30], etc.

The superconducting transition temperature, or the critical temperature, is defined as the midpoint of the transition, with the sheet resistance R_{sheet} being 50% of the normal state [28,31]. According to the measurement of the temperature dependence of γ ($\gamma - T$), this improvement of the finite MCA coefficient close to T_c can be quantified by Eq. 3 as the ratio of MCA in the resistive superconducting region (γ_S when $T \gtrsim T_c$) to the one in the normal region (γ_N) [28].

$$\frac{\gamma_S}{\gamma_N} \backsim \left(\frac{\varepsilon_F}{\Delta}\right)^3 = \left(\frac{\varepsilon_F}{k_B T_c}\right)^3 \tag{3}$$

The analysis of this MCA coefficient enhancement ratio far below T_c (or deep in the superconducting region, which will be mentioned hereinafter) involves many exotic but complex phenomena, the dynamics of vortices as an example, which is currently not so well established [26,28].

For SDE at lower temperatures ($T \ll T_c$) in the superconducting region, however, the nonreciprocity of the supercurrent cannot be studied by measuring DC resistance due to the zero value in the superconducting phase regime; hence, kinetic inductance measurements are conducted to study the supercurrent response to the AC excitation. Such superfluid stiffness can be described by an equation analogous to Eq. 2 as

$$L(I) = L_0\left[1 + \gamma_L(\boldsymbol{B}\times\boldsymbol{z})\cdot\boldsymbol{I}\right], \tag{4}$$

where the kinetic inductance response L is expected to be related to the coplanar field $\boldsymbol{B}$ and the current $\boldsymbol{I}$ under broken symmetry along the $\boldsymbol{z}$ axis. In this case, the coefficient γ_L quantifies the MCA and gives rise to the nonreciprocal phenomenon. Baumgartner et al. [32] have proposed Eq. 4, measured the kinetic inductance of synthetic noncentrosymmetric Josephson junction-based arrays, and demonstrated such supercurrent rectification far below the transition temperature, that is, $T \ll T_c$.

Before moving on to the application of logic devices based on SDE, it is instructive to highlight and optimize the potential impact parameters related to the efficiency of SDE, hence reaching a better performance for designing diode devices. First, the ratio of the MCA coefficient γ_S/γ_N, viz. the rectification ratio, which has been explicitly provided in the prior context (Eq. 3), can serve as an indicator to compare the effectiveness of rectification, thus confirming a valuable application. Additionally, from another point of view, other than the resistance transition, such nonreciprocity is also reflected in the supercurrent in noncentrosymmetric superconducting structures as well as Josephson junctions, that is, the correlation between the critical current and the direction of the current flow (see the right sketch in Fig. 2B) [32–37]. If the critical currents of different flow direction $j_{c\pm}$ are distinct from each other, viz. $j_{c+} \neq |j_{c-}|$, an SDE emerges when the applied electric current j_{ex} is between $|j_{c-}|$ and j_{c+}. The diode efficiency η, or the superconducting diode quality parameter, can thus be quantified by

$$\eta \equiv \frac{\Delta j_c}{2\overline{j_c}} = \frac{\left(j_{c+} - |j_{c-}|\right)}{\left(j_{c+} + |j_{c-}|\right)} \tag{5}$$

where the SDE is identified with a finite nonreciprocal component Δj_c of the heterostructure [36,38]. The term $\overline{j_c} = \left(j_{c+} + |j_{c-}|\right)/2$ in the denominator is defined as the averaged critical current. Apart from the fact that the breaking of the inversion symmetry is highly correlated with the strength of SOI, recent theoretical studies indicate that the strength of η can also be influenced by the applied magnetic field, temperature, disorder, etc., as shown in Fig. 3 [36,38–40]. Given all relevant system parameters but in the absence of disorder, Ilicć and Bergeret [36] have theoretically predicted a very strong diode effect, with the nonreciprocity exceeding 40% at optimal parameter regimes.

However, by extending theoretical analysis in the ballistic limit to a much more complicated occasion, the introduction of disorder mixes the two competing helical bands in a Rashba superconductor, which prefer opposite modulation vectors of

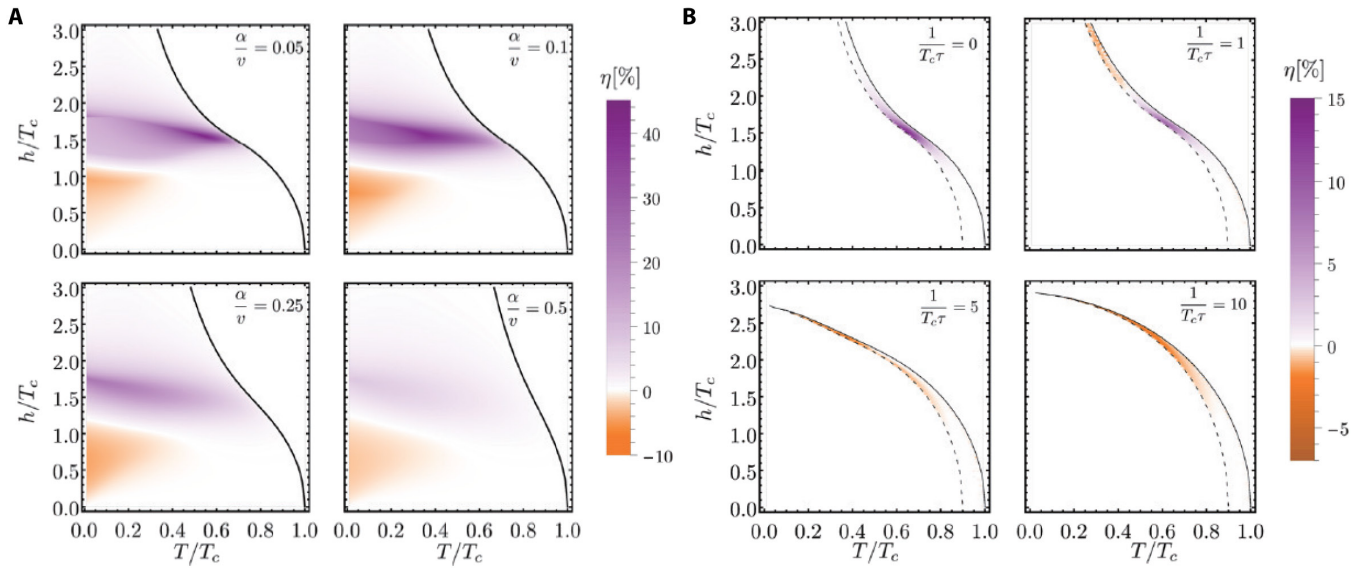

Fig. 3. The diode efficiency η for a ballistic superconductor without (A) or with (B) considering the influence of disorder. (A) The diode efficiency η was calculated for each point in the *h*-*T* phase diagram at different strengths of spin–orbit coupling denoted by α/v. The black lines show the upper critical field h_{c2}. (B) In the Ginzburg–Landau regime, considering the presence of disorder, the efficiency of the diode was calculated at various strengths of disorder while keeping α/v fixed at 0.1. The black lines here also show the upper critical field $h_{c2}(T)$, while the dashed lines meet the superconducting order condition $\Delta(T) = T$. The area between the two lines is the region of validity of the Ginzburg–Landau theory, where $T > \Delta$ [36].

the superconducting order parameter under an external magnetic field, and the increase of disorder suppresses such competition, thus leading to a weakened diode effect [36]. Also depicted in Fig. 3B, the diode efficiency undergoes a transition from positive to negative as the disorder intensifies, indicating a shift from the "strong" to the "weak" helical phase, which is considered to be the underlying cause [36].

In the initial proposition concerning the temperature dependence of [38,39], based on the Ginzburg–Landau theory, certain key factors were overlooked, namely, the intrinsic modulation of the helical phase and an additional phase gradient caused by the flowing supercurrent. Consequently, a nonzero SDE was identified at low field strengths ($B \ll B_p$) and near the critical temperature. However, this estimation was found to be overestimated and, in reality, the SDE vanishes to linear order in the magnetic field (refer to Fig. 3A) [36,38–40]. However, as the temperature T further decreases, the diode efficiency starts to increase dramatically. It is also found that both magnetic field and SOI are required for the diode effect, which break the inversion and time-reversal symmetries, respectively, and are also related to the two competing helical bands. If either magnetic field or SOI far outweighs the other, such competition will also be suppressed, leading to a weakened diode effect. Moreover, such nonreciprocal effect, denoted by critical current, shows sign reversals upon increasing the magnetic field [36,38,39]. Therefore, all these relevant impact parameters should be taken into account carefully while engineering applicable superconducting diodes.

Generally speaking, from the device fabrication's perspective and especially given the differences in internal mechanisms, SDEs observed so far can be briefly classified into two main categories, namely, noncentrosymmetric thin-film [34,41–50] or junction-based structures [32,35,51–56] corresponding to the traditional symmetric semiconductors or asymmetric semiconducting pn junctions, respectively (see Fig. 2A). Earlier theoretical works proposed by V. M. Edelstein highlighted this SDE in unconventional polar superconductors, scilicet, for the noncentrosymmetric junction-free superconductor thin films; the critical current I_{c+} and I_{c-} should be different according to the opposite flow directions, as we mentioned above [33]. In addition to the unequal critical current ($I_{c+} \neq I_{c-}$), however, the SDE in Josephson junction features another nonreciprocal phenomenon [32]. The current–voltage (*I*-*V*) characteristic of the junction with finite capacitance can be hysteric for the critical return sweep current $I_{r\pm}$, thus manifesting as direction dependence when $I_{r+} \neq I_{r-}$ [32,52].

Noncentrosymmetric thin film- and Josephson junction-based SDE

Thin film-based SDE and application

SDE may occur in noncentrosymmetric thin films when the time reversal invariance is broken by an external magnetic field. The first observation of SDE in an artificial superlattice $[Nb/V/Ta]_n$ without a center of inversion by Ando et al. [34] leads a new way toward the development of superconducting logic devices, especially enlightening the search for materials combinations with nonreciprocal transport ability in Rashba systems. The spatial inversion of a Rashba superconductor is uniaxially broken along the z axis due to the natural Rashba SOI, so the break of the time-reversal symmetry, along the y axis by the external magnetic field B_y as an example, will lead to spin reversion depending on the relative directions to the external magnetic field and a nonlinear response of current I_x proportional to the square of the electric field along the x axis (according to Eq. 2 and see Fig. 4A and B) [34]. Based on Ando et al.'s work, Narita et al. [43] fabricated noncentrosymmetric FM/SC multilayers $[Nb/V/Co/V/Ta]_{20}$ and demonstrated the unique behavior of magnetization-mediated nonreciprocal SDE without the need for an external magnetic

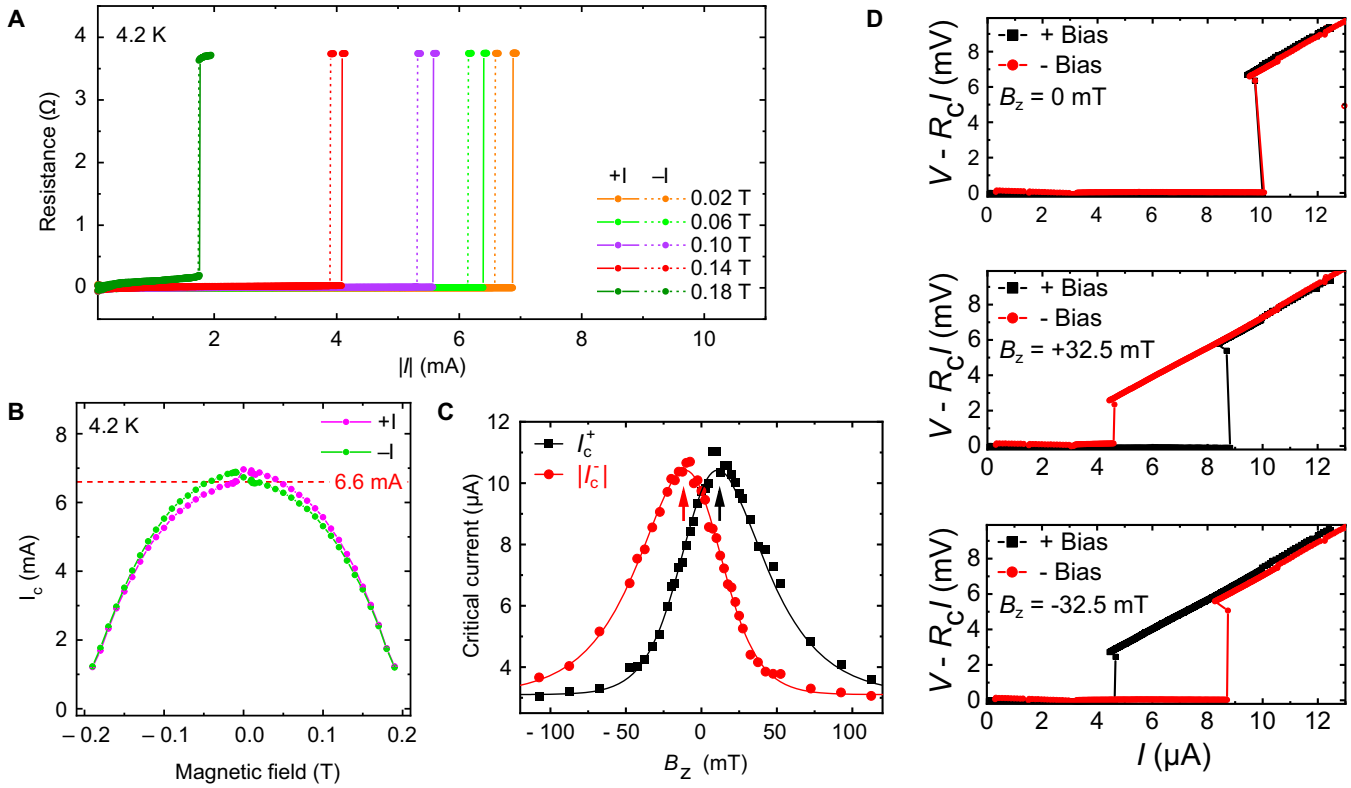

Fig. 4. (A and B) Asymmetric *R-I* curves under various magnetic fields for both bias flow directions $I_{\pm}$ and the nonreciprocal I_c as a function of the magnetic field in the $[Nb/V/Ta]_n$ superlattice, respectively [34]. (C and D) SDE in a van der Waals superconductor $NbSe_2$ within which the breaking of time reversal symmetry is attributed to Ising-type SOI. (C) *I-V* characteristics for opposite flow directions $I_{\pm}$ under various out-of-plane field B_z. (D) Nonreciprocal critical current as a function of B_z. Critical currents reach maximum for a nonzero B_z around 10 mT, indicated by black and red arrows [44].

field. A more recent experimental study from Hou et al. [57] demonstrated strong SDE in conventional thin-film Pt/V/EuS with a giant SDE efficiency of 65% under small 30 Oe (21% below zero). The ubiquitous SDE in thin-film superconductors from this work even without the need for spin–orbit or direct exchange coupling indeed challenges the prevalent verification method of using the SDE as a proof of finite–momentum pairing [57]. Further research is still needed for convincing clarification.

Usually, superconductivity is suppressed when the magnetic field exceeds the paramagnetic limiting field (or referred to as the Pauli limiting field) due to the Zeeman splitting of the spin degenerate states at the Fermi level, but in the Ising type superconductors, things are much more tricky due to a very different intrinsic origin [45,46]. Similar to but different from the Rashba (or Dresselhaus) type, the breaking of in-plane inversion symmetry in this kind of superconductors leads to the emergence of Ising-type spin–orbit coupling, which provides a new pathway for the application of superconducting devices in strong magnetic fields. Recent discovery from Bauriedl et al. [44] has recognized such a considerably larger supercurrent diode effect (see Fig. 4C and D) compared to its normal Rashba similitudes with a rectification efficiency of up to 60% in exfoliated $NbSe_2$ crystal multilayers, providing the possibility to investigate the construction of superconducting diode devices using novel materials with different types of spin–orbit coupling effects.

Josephson junction-based SDE and application

In addition to bulk, thin-film, or engineered heterostructures, Josephson junction-based structures may serve as another important component for designing superconducting logic devices similar to their semiconductor counterparts, such as Schottky contacts and semiconductor p–n junctions. Also, compared with the conventional superconductivity of multilayer devices, which can be strongly suppressed by the proximity effect between the competing superconducting and ferromagnetic layers, Josephson junctions can be easily regulated by the barrier layers as well as the extrinsic, external magnetic field as an example. Theoretical expectations for the emergence of a Josephson diode [51,52] were met with the groundbreaking experimental discovery in 2022. This involved the observation of a sizable SDE within Josephson junctions. The approach utilized an epitaxial aluminum (Al) layer to proximitize an InAs two-dimensional (2D) electron gas well below the transition temperature, paving the way for the creation of innovative dissipationless circuit elements [32]. As shown in Fig. 5, the breaking of both spatial inversion and time reversal symmetries leads to the broken Kramers degeneracy between the two spin components, thus showing asymmetric behavior of the current phase relation (CPR) around the inflection points (i^*,φ^*). Both field direction-dependent inflection points and phase difference-dependent extremal values (viz. critical currents $I_{c\pm}$) are correlated with the supercurrent diode effect, with superflow in only one direction. Subsequent work has proposed alternative material combinations for the development of such diode devices [32,53]. However, most of these diode devices based on SOI require the application of an external magnetic field to break the time reversal symmetry via Zeeman spin-splitting [54].

The essential external magnetic field indeed restricts practical application due to additional energy loss; hence, the spontaneous idea of using intrinsic magnetization can serve as a

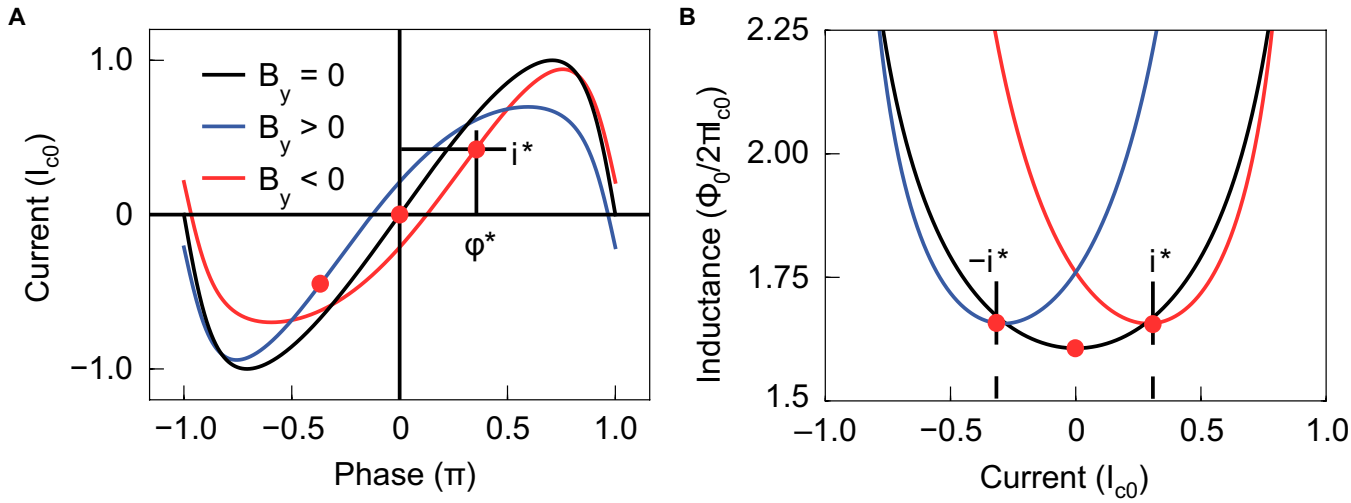

Fig. 5. (A) The current phase relation was examined for a short-ballistic Josephson junction with high transparency and a robust spin–orbit interaction (SOI), both in the absence and presence of a transverse magnetic field B_y. Results are depicted as red curves for $B_y > 0$ and blue curves for $B_y < 0$. In this example, the effect of finite $\pm B_y$ indeed twists the original CPR curve by reducing the critical current and adding a cosinusoidal term to the CPR's Fourier series. The red dots denote the inflection points (i^*, φ^*) of the CPR. (B) Corresponding Josephson inductance as a function of current [32].

substitution, leading to a heated discussion on searching field-free Josephson diodes from van der Waals heterostructures [35], proximity-magnetized barrier [54] to magnetic dots [55], etc. Specifically, the prototypes of cross-like planar Josephson junctions equipped with supplementary electrodes and an artificial vortex trap reported at zero field by Golod and Krasnov show the maximum rectification efficiency (exceeding 70%) to date [56]. Such diode device showcases remarkable tunability, achievable by altering the bias configuration and manipulating the presence or absence of a vortex, which may also be used for memory application capable of in-memory computing paradigm.

General SDE in unconventional superconducting structures

The superconducting proximity effect, one of the most central topics in the research of superconducting spintronics, is also currently being investigated in unconventional superconducting materials like graphene [42,58], topological semiconductors [59], and topological insulators (TIs) [60,61] to yield topological superconductivity.

For example, as a prototypical 2D quantum system, graphene possesses a highly appealing feature for spin-based applications due to its low SOI, resulting in prolonged spin lifetimes [2]. Furthermore, the incorporation of graphene as an interlayer can significantly enhance the efficiency of spin injection at the FM/Si interface [62].

Recent studies of superconducting heterojunctionsand diodes in magic-angle twisted bilayer graphene [58] and small-twist-angle trilayer graphene [42,63] indeed envision such nonreciprocal diode effect.

Pal et al. [59] reported a giant and maximum Josephson diode effect in Josephson junctions constructed using $NiTe_2$, a typical type II Dirac semi-metal, in the presence of a slight in-plane magnetic field perpendicular to the supercurrent.

In addition, the interaction between the symmetry protected surface states of TI and broken symmetry states in magnets and SCs can lead to time-reversal invariant topological superconductors (TSCs) [64], thus offering a new pathway for the application of superconducting spintronics, among which both topological superconductors [60,61] and topological Josephson junctions [59] can serve as promising components in topological quantum information processing and in dissipationless logics through the creation of superconducting diodes.

The nonreciprocal diode effect has long been investigated in noncentrosymmetric low-dimensional superconductors and Josephson junctions [28,30,65–67]. For instance, Wakatsuki et al. [28] experimentally demonstrated such nonreciprocal diode effect with a quite large rectification ratio of five orders of magnitude. Gupta et al. [65] reported the observation of the Josephson diode effect in a three-terminal Josephson device based on an InAs 2D electron gas proximitized by epitaxial Al, which can be switched between positive and negative polarity by electrostatic gating. Furthermore, de Picoli et al. [66] theoretically presented a nonreciprocal behavior of the critical current in quasi-1D systems and provide a complementary description to Ginzburg-Landau theories of such diode effect. Nevertheless, more recent experimental investigations have further advanced the exploration of current-biased Josephson junctions, revealing diode-like characteristics with the incorporation of a solitary magnetic atom. This intriguing phenomenon may be attributed to a novel mechanism that involves asymmetric quasiparticle damping, which obviates the need to break the time-reversal symmetry through an externally applied magnetic field [67].

Cryogenic Superconducting Memory Technologies

Given the widespread use of von Neumann architecture in current computing systems, where the processor and memory are physically separated, the continuous movement of data is increasingly becoming a critical bottleneck for both data transfer bandwidth and power consumption reduction. Various solutions have been proposed to complement traditional computer memory systems, depending on different application

scenarios, ranging from data-centric computing paradigms to disaggregated storage schemes. The implementation of alternative technologies, such as superconducting devices, beyond traditional silicon-based CMOS technology has garnered significant attention in data- or energy-intensive HPCs and data centers. However, due to the spin-related superconducting logic devices mentioned above, cryogenic memory technologies must also be compatible with the extremely low-temperature (4 K or below) working environment. In this section, we discuss both cryogenic nonsuperconducting memories and superconducting memories, exploring their intrinsic mechanisms, recent advancements, and future applications.

Nonsuperconducting memory technologies

DRAM [68] is a kind of conventional semiconductor memory that incorporates the charge stored in a capacitor to interpret binary bits as 1 or 0. However, due to the unavoidable leakage current in nonsuperconducting transistors, which are especially affected by the ever shrinking dimensions as well as high-density integration of transistors, periodic charging is extremely required in DRAM to compensate potential data loss, making it a "dynamic" device. Recent research indicates that CMOS circuits exhibit better performance at 4 K compared to room temperature (RT) [69]. The increasing mobility along with the decreasing temperature in this case surpasses the compensatory threshold voltage increase, thus, leading to great enhancement in both transistor switching speed and drive current at lower temperatures. General DRAM-based devices are considered comparable to conventional logic technology and are expected to perform well at 77 K and above [70,71]. In 2014, HfO_X-based resistive random access memory or with an Al_2O_3 layer between HfO_X and the bottom electrode was chosen for its self-compliance characteristics [72]. By leveraging the enhanced subthreshold slope and minimizing junction leakage, optimized DRAM can substantially decrease threshold and operating voltage, resulting in reduced power consumption while preserving performance.

Static random-access memory (SRAM) is a type of random-access memory. The term "static" implies that data stored in this memory remains intact as long as it is powered on. In contrast, data stored in DRAM requires periodic refreshment. However, when the power supply is interrupted, data stored in SRAM is lost (referred to as volatile memory). This is distinct from flash memory, which can retain data even after a power failure.

As microelectronics technology advances rapidly, SRAM is evolving toward higher integration, increased speed, and lower power consumption. The rising supply voltage (V_{dd}), threshold voltage (V_{th}), and wire resistance present significant challenges to the logic integration of SRAM [73–75]. In 1987, researchers discovered that operating MOSFETs at liquid nitrogen temperature (77 K) offered considerable reliability advantages [76]. Cryo-CMOS, which leverages these advantages at both the device and system levels, provides higher carrier mobility, reduces junction leakage, sharpens V_{dd} transitions, lowers interconnection resistance, and minimizes current thermal losses. These features effectively address the challenges mentioned above [77,78]. Hu and Liu [73] decreased the static noise margin (SNM) of cryo-CMOS SRAM from 39.6% to 11% when operating at 77 K, as compared to RT. In the same year, another group of researchers reported substantial reductions in read noise at 77 K compared to 300 K. Moreover, data retention characteristics improved by a factor of 3, and cycle endurance increased by about 10-fold at 77 K compared to 300 K. When evaluating the cooling cost and bit cost scaling in relation to workload duty, they found that SRAM, with its relatively extended standby time and limited workload, is ideally suited for cryogenic operation due to its associated lower cooling costs [74]. In 2008, Barlow et al. [79] presented the design of an SRAM block intended for extreme environmental applications, such as robotic and human explorations on the Moon and Mars. This SRAM block was designed to operate reliably under extreme conditions, including temperatures as low as −180°C during lunar nights and −230°C in the shadowed polar craters, aligning with NASA's planned lunar missions.

In addition to its applications in quantum computing and aerospace electronics, cryogenic operation can also be readily employed to enhance storage performance. This leads to noteworthy improvements in storage capabilities, including reduced read (verify) noise, extended data retention, and increased cycle endurance.

MRAM, on the other hand, stands out as a highly promising contender for the next-generation nonvolatile memory technology, which utilizes a free layer and a fixed layer to store information based on relative magnetization configurations [80,81]. In the parallel state (P), the resistance is low ("0" as an example), whereas in the antiparallel state (AP), the resistance is high ("1" as an example). The memory reading circuit determines the information stored in the memory by applying the same voltage and measuring the magnitude of the output current. Recently, MRAM has gained recognition for its potential application in leading-edge superconducting computer architecture [20,82]. The investigation of CoFeB/MgO-based perpendicular magnetic tunnel junctions (pMTJs) at low temperatures, for example, involved analyzing their quasi-static switching voltage, high-speed pulse write error rate (WER), and endurance at low temperatures, specifically down to 9 K [83]. At this temperature, the devices exhibited endurance that exceeded that at 300 K by three orders of magnitude, enduring over 10^{12} cycles with 10-ns write pulses under the same write conditions. Garzón et al. [84] investigated double-barrier STT-MRAM with two reference layers operating at cryogenic temperatures (Fig. 6). The research achieved a 2-MB DMTJ-based STT-MRAM operating at 77 K, which improved accessing time by 28% and reduced both read and write energy consumption by 52% and 38%, respectively.

In 2019, researchers reported the properties of spin-transfer switching with nanosecond duration at low temperatures in pMTJ nanopillar devices and compared them to their RT performances. While the switching energy increases as the temperature decreases, it still remains significantly favorable compared to other types of spin-transfer devices at 4 K. As shown in Fig. 6, the device exhibits a faster switching at 4 K than at RT for both switching directions, from P to AP or from AP to P. Furthermore, error rate measurements demonstrate high reliability, with $WER \leq 5 \times 10^{-5}$ using 4-ns pulses at 4 K [82].

Superconducting memory device

In superconducting spin valve devices, the two superconducting layers sandwich the ferromagnetic layers and the exchange field from the ferromagnetic layers can in turn influence the electron pairing from the adjacent superconducting layers, consequently inhibiting the superconducting properties. Through manipulation of the magnetization orientations in the ferromagnetic layers, it becomes possible to modulate the superconducting

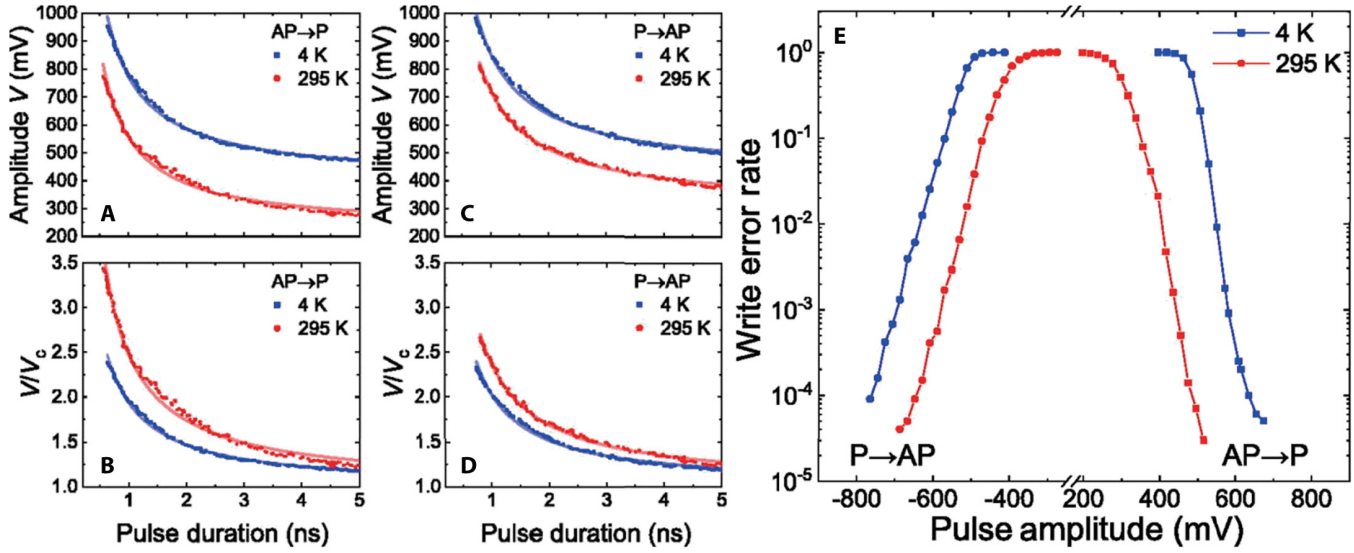

Fig. 6. (A to D) Switching process of parallel and antiparallel states at both 4K and RT. Blue lines indicate that shorter pulse times are required at the same overdrive V/V_c or amplitude. In (E), the WER for 4-ns duration pulses is illustrated at both 4 K and 295 K temperatures. Notably, the low-temperature WER at the same pulse amplitude is 10 orders of magnitude larger than at RT. These measurements were carried out on a 40-nm-diameter pMTJ nanopillar [82].

critical current, providing a method for information storage. In Josephson junction-based superconducting memory devices, information is stored through magnetic flux. Compared to superconducting spin valve devices, the Josephson junction comprises two superconducting layers separated by a thin insulating barrier, where a magnetic field can induce a phase difference between the two, leading to a change in the critical Josephson current (I_c).

Superconducting spin valve

The critical temperature of the superconducting layer in FM_1/SC/FM_2 structures in superconducting spin valve configurations is contingent upon the relative magnetization orientation of the two ferromagnetic layers [85]. Moraru et al. [86] observed a difference in the T_c of the superconducting layer between the P and AP configurations of the two outer ferromagnetic layers, as wide as 41 mK in Ni/Nb/Ni and CuNi/Nb/CuNi sandwich structure. They also measured ΔT_c in the trilayer structure using permalloy (Py = $Ni_{84}Fe_{16}$) as a strongly polarized ferromagnetic material, which was found to be 20 mK. In metallic superconducting spin valves, due to the superconducting proximity effect, Cooper pairs could partially transmit to the nearby ferromagnetic layer through Andreev reflection, resulting in an additional decrease in ΔT_c. This may be the reason why ΔT_c is difficult to increase. In 2013, Li et al. [87] reported that they used a ferromagnetic insulator (EuS) (Fig. 7) as the FM layer to restrict the Cooper pair transmitted to adjacent layers (Al). The thickness of Al is much less than the coherence length ξ_s ($\xi_s \approx 79$ nm) [88] due to the fact that the intrinsic superconductivity of the Al film is influenced by the stronger exchange field of the magnetic rare earth metal ion (Eu^{2+}) as well as the P or AP configuration of the magnetic moments [85]. The magnetic resistance is defined as $MR = ((R_{max} - R_{min})/R_{min}) \times 100\%$, where R_{max} and R_{min} are the resistances of P and AP depending on the relative magnetization configuration. On the basis of the infinite magnetoresistance when changing from the resistive state to the superconducting state, the proposed magnetic superconducting memory cell can achieve complete switching of the superconducting state to increase the storage window and provide a solution for the comprehensive performance optimization of cryogenic memory. Similar structures can also be implemented using the GdN/Nb/GdN and Ho/Nb/Ho systems [89,90].

Magnetic Josephson junction

The Josephson junction, also known as the superconducting tunnel junction, is a structure typically composed of two superconductors separated by a very thin barrier layer, with a thickness smaller than the coherence length of the Cooper pairs. The structure can be represented by an S/I/S configuration, in which superconducting Cooper pairs can tunnel through an insulating film from one side to the other [11]. This phenomenon was first predicted by Brian Josephson and later experimentally confirmed by Anderson and Dayem [91]. In 1988, Tahara et al. [92] demonstrated a vortex transitional nondestructive readout Josephson memory cell that consisted of two superconducting loops in which a single flux quantum is stored and a two-junction interferometer gate is combined as a sense gate. They achieved a ±21% address signal current margin and a ±3% sense gate current margin experimentally. However, due to the data explosion brought about by the post-Moore law era and the need for storage systems for superconducting computers, the storage capacity of SIS-JJ-based memory is gradually becoming overwhelmed [93–97]

Magnetic Josephson junctions (MJJs) are devices in which a magnetic barrier is sandwiched by two superconducting electrodes, creating a SC/FM/SC junction, where novel physics emerge due to the interplay between superconductivity and magnetism. In an MJJ device, the strong exchange effect of the ferromagnetic layer penetrates the superconducting layer, causing the momentum and wave function phase of spin-up and spin-down electrons in Cooper pairs to change. As a result, the phases of the order parameter are separated into 0 or π state [98]. This effect is especially pronounced when the thickness of the ferromagnetic barrier is approximately a half-integer multiple of the oscillation period, leading to a distinction in the signs of the order parameters in the two superconductors

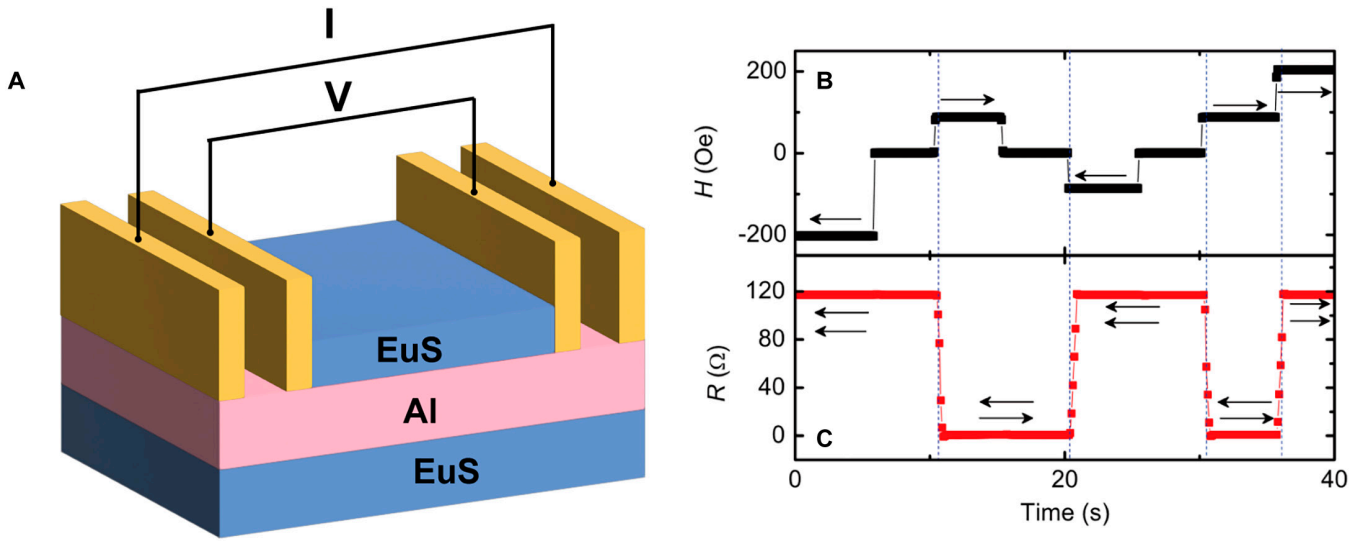

Fig. 7. (A) Schematic view of the EuS (1.5)/Al (3.5)/EuS (4) device structure. (B and C) Gradual increase and decrease, respectively, of the applied magnetic field over time. These changes in the field result in corresponding variations in the measured resistance (C) of the EuS/Al/EuS trilayer at a temperature of 1.2 K. The resistance of the trilayer device exhibits switching behavior between a high-resistance state and a low-resistance state, allowing the realization of "0" or "1" writes. The arrows depicted in the figures indicate the orientations of the magnetic moments in the two EuS layers, highlighting the magnetization orientation within the trilayer structure [87].

[15,72]. Researchers have applied an external magnetic field to affect the magnetization of the ferromagnetic layer to change the critical current (I_c) of the junction, with the structure of superconductor/insulator/superconductor/ferromagnet/superconductor Nb/Al(AlOx)/Nb/PdFe/Nb. This modification allows two distinct states to be realized with high and low I_c denoting logic "0" or "1" (Fig. 8) [99]. A small magnetic field, which can be easily achieved by the Helmohltz coils, can perform the nonvolatile change of I_c of the MJJ-based memories.

For MJJ memory applications, it is crucial that the amplitude of the critical current (I_c) or the $0 - \pi$ phase shift [15] across the junction be controllable by changing the magnetization direction of one or more of the ferromagnetic layers in the junction. Engineers at Northrop Grumman Corporation further developed superconducting memory devices based on the JMRAM concept. Subsequently, Niedzielski et al. [100] designed a multi-FM-layer structure $SC/FM_1/NM/FM_2/SC$ to control the critical current or phase shift by changing the relative magnetization orientations of the FM layers. Research suggests that switching the magnetization direction of the soft ferromagnet allows for switching the critical current between high and low. Then, by ingeniously choosing the thickness of the FM layers, it should be possible to switch the junction between 0 and π states. However, the thicknesses of both hard and soft ferromagnetic layers must be controlled very precisely, because Cooper pair correlations oscillate and decay very fast even in the ferromagnetic layers, especially exceeding the decay length of FM, which is not a very useful range from the application point of view [99–102].

Overall, the review presented here highlights the potential of MJJs in the development of cryogenic memory devices for quantum computers and SFQ systems. However, there are still two challenges that need to be addressed for practical applications of MJJ-based memory devices. First, a more suitable magnetic layer is required to increase the coherence length of superconducting Cooper pair transmission and prevent excessive loss from superconducting current in the magnetic layer. Second, there is a need to further increase the regulation amplitude of the critical current (I_c) to enhance the storage window. Solving these challenges could lead to significant advancements in the development of high-performance cryogenic memory devices using MJJs.

Superconducting spintronics memory

Since the discovery of superconducting heterostructures, significant attention has been focused on utilizing traditional low-temperature superconductors, such as Cooper pairs, to achieve phase coherence and nonlocal entanglement between electrons. Substantial progress has been made in this field. In particular, ferromagnetic Josephson junctions (SC/FM/SC) offer a unique platform for integrating the coherent quantum properties of superconductors and ferromagnets, enabling unconventional mechanisms and smart tunable functionalities. Simultaneously, researchers have also begun to explore the long-range transport of spin flow in heterostructures.

In this part, our objective is to introduce the methods employed for long-distance transmission in devices. The review will encompass a discussion on the research progress of superconducting spintronics in SC/FM heterostructures, including topics such as SC quasiparticles, spin-triplet spin valves, and spin-triplet Josephson junctions.

Superconductor quasi-particles for superconducting spin valve (SSV)

Superconductors are highly intriguing for spin injection experiments because of their ability to achieve nearly complete spin polarization, extended spin relaxation times, and distinct segregation of spin and charge properties. Therefore, the study of superconducting spintronics has focused on finding a material system with a long spin lifetime. Early research in this field relied on the spin polarization of superconducting quasiparticles, which were predicted to have a long spin lifetime. As Fig. 9 shows, superconducting quasiparticles are low-energy single-fermion excitations in superconductors that can be viewed as coherent superpositions of electrons and holes [103]. The spin diffusion length of quasi-particles in FM/SC/SC was

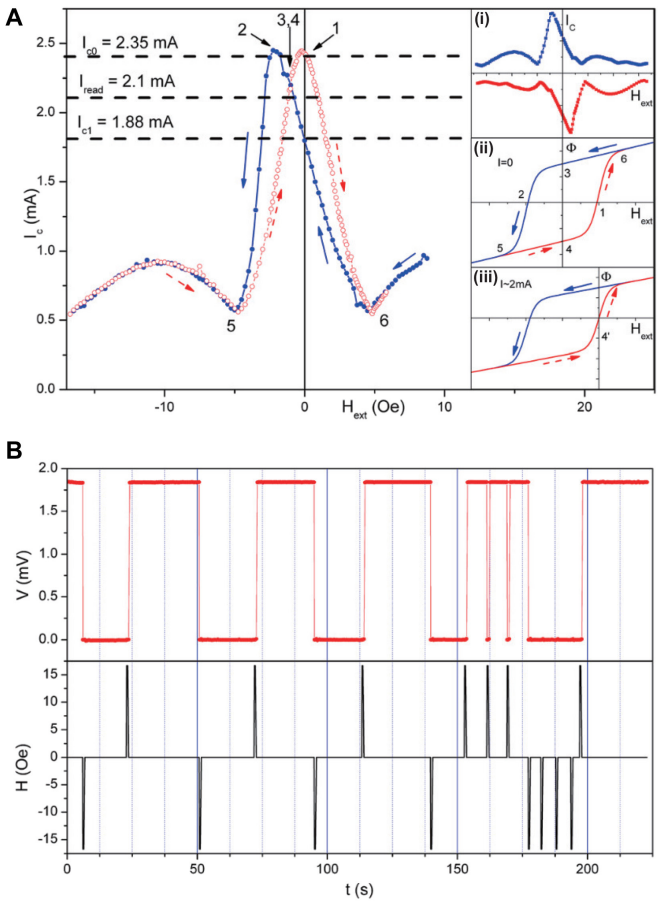

Fig. 8. (A) $I_c - H$ curve of an SFQ device. In (i), a symmetric curve is displayed, showcasing the maximum critical current at a nonzero extra field. (ii and iii) Hysteresis loops in relation to the external field. In (ii), the bias current is set to zero, while in (iii), a current close to I_c is applied to the device. The arrows indicate the directions of the magnetic field sweep. (B) Positive and negative magnetic field pulses are applied to switch the superconductor/insulator/ferromagnet/superconductor junction between a superconducting state (zero resistance) and a resistive state, and vice versa. (B) Positive and negative magnetic field pulses are applied to switch the junction between a superconducting state (zero resistance) and a resistive state, and vice versa [99].

detected by Joule heat generated at the Josephson junction theoretically [104]. Al is a more common superconductor that produces quasi-particles. In 2010, Yang et al. [105] experimentally observed extremely long spin lifetime of SC quasiparticles for the first time. In an MTJ-like structure (IrMn/CoFe/MgO(Al)/CoFe), they discovered that spin-polarized quasiparticles within superconducting Al layers exhibit remarkably prolonged spin lifetimes, nearly a million times longer compared to their normal state. The thin Al layer was embedded within an insulating MgO layer, and the spin lifetime was determined by observing the suppression of superconductivity in Al due to the accumulation of spin-polarized carriers in the superconductor layer using tunnel spin injectors. When in the superconducting state, the Cooper pair condensate is composed of spin singlets, resulting in a total spin of zero in the absence of spin–orbit scattering. Nevertheless, the presence of SOI renders spin an unreliable quantum characteristic. Under the influence of a slight external disturbance, for instance, electrical spin injection or a magnetic field, specific Cooper pairs are virtually stimulated, resulting in the generation of quasiparticles possessing nonzero spin. As a consequence, a finite spin susceptibility emerges, and spin accumulates at low temperatures, resulting in an exceptionally prolonged spin lifetime within the superconducting state. A similar charge-spin separation property that enhances the spin lifetime in superconducting Al has also been reported by Quay et al. [106] based on the lateral spin valve structure with $Co/Al_2O_3/A_l/Al_2O_3/Co$.

Recently, researchers have started to apply this phenomenon to practical applications. One such application is the superconducting spin-valve effect. Attributed to either quasiparticle spin-accumulation suppressing T_c in the AP or flux penetration in the superconducting layer from out-of-plane domain walls in the ferromagnetic layers, devices with suitably large ΔT_c and infinite magnetoresistance held at constant temperature have been reported. A previously reported device using current-perpendicular-to-plane (CPP) geometry was an FM/SC/FM spin valve, which shows giant magneto resistance (GMR) behavior due to quasiparticle transport with a reduced spin decay length relative to the normal state for superconducting Nb layer thicknesses exceeding 30 nm [107]. The attainment of a critical thickness is of utmost importance in the advancement of industrial devices for quasiparticle spintronics. It implies that in order to

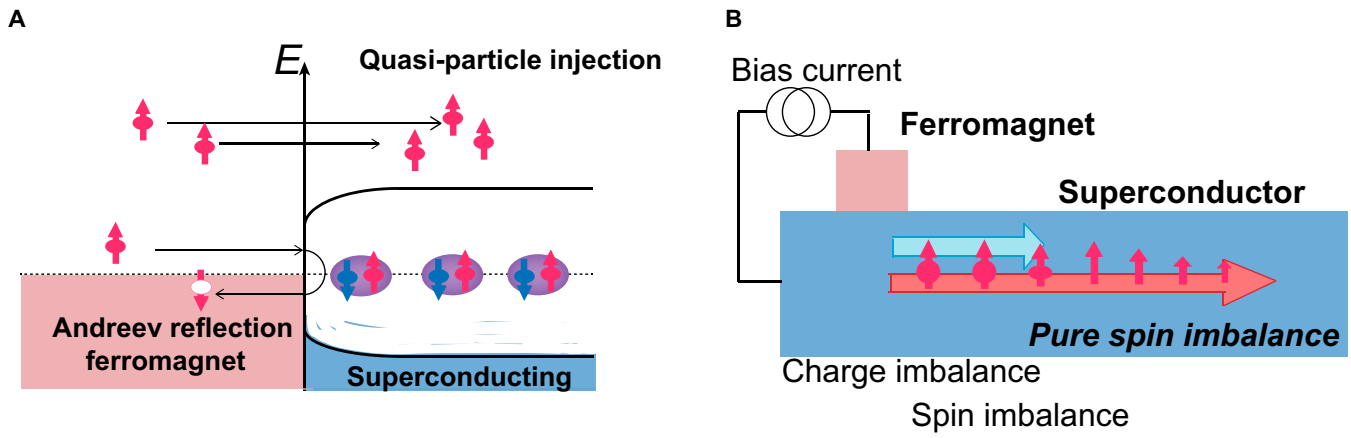

Fig. 9. (A) Concepts of Andreev reflection and quasi-particle injection at a FM/superconductor interface. In the case of singlet pairs in a superconductor, they cannot carry a net spin-angular momentum due to the conservation of spin-angular momentum. Consequently, in order to introduce spin-polarized electrons into a superconductor, they are injected as quasi-particles. (B) Only spin information is propagated in a pure spin current, while the charge remains localized or unaffected [123].

fabricate devices that harness quasiparticle effects effectively, it is advisable to employ Nb thicknesses greater than 26 nm or explore the use of the superconducting spin-valve effect. An example of this is the improved preservation and manipulation of information (or entanglement) encoded in long-lived spins when superconducting Al is employed in quantum computing memory devices.

Spin-triplet device

Triplet SSV: The Lorentz force manifests distinct effects on Cooper pairs with opposite internal spins when subjected to a magnetic field. The co-alignment of spins is facilitated by the Zeeman interaction and magnetic field, leading to spin-flip phenomena caused by the energy instability of electrons under strong magnetism. While Cooper pairs in conventional s-wave superconductors dominate dissipationless charge current, they are not typically considered capable of carrying dissipationless spin current because of the zero-spin angular momentum carried by spin-singlet Cooper pairs. This arises from the odd parity of pairing between spin-up and spin-down electrons ($|\uparrow\downarrow> - |\downarrow\uparrow>$).

However, at the S/F interface, the singlet Cooper pair experiences a spin-dependent phase shift of the electrons, with acquisition of a nonzero center of mass momentum. The phase shift transforms the singlet wavefunction so that it represents a mixture of singlet and triplet components [100–102,108]. Thus, the spin mixing process at the S/F generates a triplet pair component within the ferromagnet with $S = 1$ and $S_z = 0$. This triplet component, comprising an average of opposite spins, decays in the ferromagnet over the same length scale as that of the singlet component. Under certain conditions, the $S = 1$, $S_z = 0$ triplet component can be transformed into a $S = 1$, $S_z = \pm 1$ triplet component, with net spin projection. This $S_z = \pm 1$ triplet component, with the same spin ($|\uparrow\uparrow>$ or $|\downarrow\downarrow>$), is not sensitive to the ferromagnetic exchange field, and thus, its coherence length within the ferromagnet, which far exceeds the singlet case S/F, is more similar to the S/N case where decoherence results from spin-flip processes. Unlike spin-singlet superconductors, which are significantly influenced by the exchange field of a ferromagnet, equal spin-triplet Cooper pairs are not constrained by ferromagnetic polarization. As a result, they can induce the superconducting proximity effect in a ferromagnet and establish long-range Josephson coupling within the ferromagnetic material.

The theoretical and experimental confirmation of this phenomenon has been observed in JJs containing multiple ferromagnetic layers, which generate spin singlets or triplets as a result of the exchange field of the ferromagnetic materials. Early in 1997, a theoretical proposal emerged for an unconventional $SC/FM_1/FM_2$ structure resembling a spin-valve configuration. This proposal aimed to regulate the superconducting critical temperature within the superconducting layer by aligning the magnetizations of the two neighboring ferromagnetic layers [109]. The model calculations have shown that the transition temperature for the AP orientation of the FM1 and FM2 magnetizations (T_C^{AP}) should be higher than the transition temperature for the opposite case (T_C^{P}). This is due to the partial cancellation of the pair-breaking exchange fields within the magnetic subsystem of FM_1/FM_2 in the structure.

On this basis, Fominov et al. [110] showed for the first time that the minimal critical temperature T_C^{TR} of the structure is achieved at a noncollinear alignment of the magnetizations. Since T_C^{TR} is lower than both T_C^{P} and T_C^{AP}, it offers the possibility of a "triplet spin valve effect." When the temperature is above the minimum T_C^{TR} but below T_C^{P} and T_C^{AP}, the system is superconducting only in the vicinity of the AP and P configurations, which is necessary to achieve logical write. The model explains that this SC/FM1/FM2 structure allows for not only the standard but also the inverse spin-switching effect. This triplet-SSV effect can serve as conducting GMR devices, for example, as MRAM elements [10]. In the investigated system, the information can be read out at zero applied field, eliminating the need for a permanent field to stabilize both states. This system also serves as a superconducting element for spintronics in MRAM. The standard or inverse spin-switching voltage effect can serve as the foundation for an MRAM. Nonetheless, it is essential for the system to possess suitable magnetic hysteresis characteristics, and the superconducting transition temperature must exhibit disparity between the two magnetic configurations achieved in the absence of an external field [22,111].

The researchers have launched various experiments and explorations in this field. Lenk et al. [112] reported $Co/CoO_x/Cu_{41}Ni_{59}/Nb/Cu_41Ni_{59}$ nanoscale thin-film heterostructure that functions as a superconducting spin-triplet MRAM element. The long-range superconducting triplet pairing component with spin-projection one, caused by noncollinear magnetic moments in the sample, enables this system to serve as a superconducting MRAM element. It can operate without requiring an external field for storage or readout of the information. It functions without the need for an external field for information storage or readout. Therefore, the introduced triplet spin valve serves as a superconducting counterpart to the conventional GMR spin valve, enabling its application as an MRAM element.

Triplet JJ: Over the course of the last 20 years, experimental investigations into ferromagnetic Josephson junctions have exhibited remarkable potential since the initial demonstrations of the renowned π junctions. There exist two distinct types of controllable phase state in MJJs. One type exhibits an inherent spin-singlet supercurrent, while the other type facilitates the conversion of spin-singlet electron pairs into spin-triplet pairs within the junction [108,113]. The superiority of spin-triplet MJJs compared to spin-valve Josephson junctions lies in their capability to transition between the 0 phase and the π phase by solely reversing the magnetization of either outer layer, FM1 or FM2, irrespective of their thicknesses. In the latter proposal, the triplet JJ consists of three magnetic layers with noncollinear magnetizations between neighboring layers. The ground-state phase difference across the junction is determined by the relative alignments of the magnetizations in all three FM layers.

Martinez et al. [114] demonstrated the capability to manipulate the magnetization direction of adjacent ferromagnetic layers in multiferromagnetic Josephson junctions, thereby exerting control over the amplitude of a spin-triplet supercurrent. The specific structure of the junctions used in this experiment was Nb(100)/Cu(5)/Ni(1.2)/Cu(10)/Co(4)/Ru(0.75)/Co(4)/Cu(10)/NiFe(1.0)/Cu(5)/Nb(20)/Au(15)/Nb(150)/Au(200). The central layers of the junctions consisted of two Co layers separated by a Ru spacer (0.75 nm), forming a coplanar synthetic antiferromagnet (SAF). This SAF layer was sandwiched between a "hard" layer (Ni) and a "soft" layer (NiFe). By manipulating the magnetization direction of the neighboring ferromagnetic layers, the researchers were able to control the amplitude of

the spin-triplet supercurrent that traversed the junctions. This study highlights the potential for manipulating spin currents in complex multilayered Josephson junction structures. Glick et al. [115] provides experimental verification from another research group, showcasing that a Josephson junction consisting of three magnetic layers with noncoplanar magnetizations exhibits a ground-state phase shift of either 0 or π. In this study, a perpendicular SAF was formed using two $[Pd(0.9\ nm)/Co(0.3\ nm)]_n$ multilayers sandwiched by a Ru (0.95 nm) layer. The observed phase shift is contingent upon the relative orientations of the magnetizations within the layers. The orientations are carefully selected to enable the switching of one layer's magnetization by 180 degrees without impacting the other two layers. Importantly, this behavior is observed even in more complex structures, such as SC/NM/FM1/NM/FM/NM/FM2/NM/SC, demonstrating the robustness of the observed phenomena in intricate setups (as depicted in Fig. 10). The ability to control the ground-state phase difference in Josephson junctions has significant potential applications in high-speed superconducting SFQ circuits and quantum computing circuits.

Based on this research, a conceptualized SQUID loop was proposed, comprising two conventional SIS-JJs and an additional ferromagnetic junction serving as a passive phase shifter [116]. Applying the appropriate current bias and flux to the memory cell allows for the straightforward detection of changes in the critical Josephson current curve of the SQUID. An advantage of this design is that only the SIS-JJ undergoes a transition to the voltage state during memory readout. By harnessing the switching of the SIS-JJ, a substantially larger signal can be generated, given that ferromagnetic junctions typically have an I_cR_N value of only a few microvolts or even less [117].

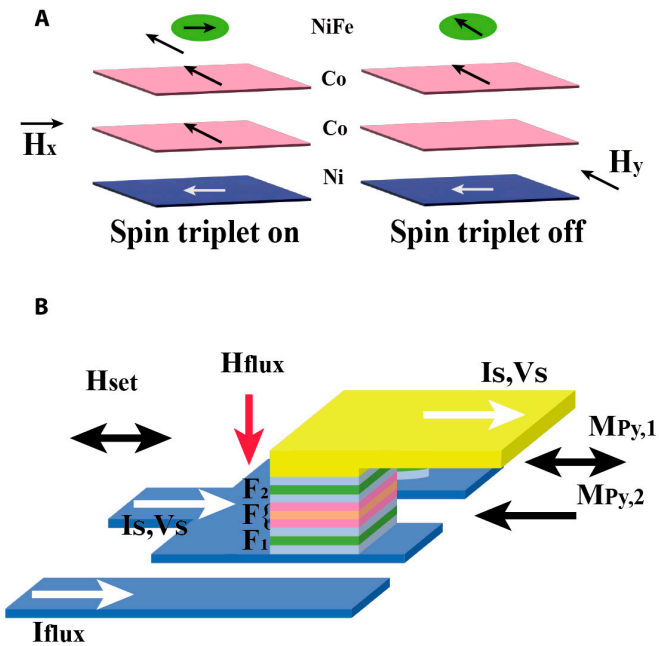

Fig.10. (A) The schematic diagram shows the structure using hard magnet (Ni)/SAF/soft magnet (NiFe). When the magnetization of the three layers in the structure is orthogonal to each other, a spin-triplet state can be generated, and the switching of the triplet state current can be further controlled by controlling the magnetization distribution of the structure [114]. (B) The schematic design of the spin-triplet Josephson junction device showcases a structure similar to an MTJ. The junction's phase behavior is explored through the construction of a SQUID. The SQUID comprises two Josephson junctions that are simultaneously fabricated, but with distinct shapes: one is elliptical, while the other is an elongated hexagon. This arrangement enables the magnetization direction of the free layer in the elliptical junction to be switched independently, without impacting any of the magnetic layers in the other junction. An applied flux, denoted as I_{flux}, induces a perpendicular field H_{flux}. $M_{Py,2}$ and $M_{Py,1}$ represent the magnetization of Py in the two nanopillars, respectively [115].

In the context of large-scale memory applications, spin-valve junctions offer the advantage of having only two FM layers, in contrast to the three present in multi-ferromagnet Josephson junctions. Nonetheless, it is crucial to carefully select the thicknesses of the FM layers in spin-valve junctions to maintain an acceptable range. In contrast, spin-triplet junctions impose less strict limitations on the thicknesses of the FM layers, rendering them more suitable for large-scale industrial production. Furthermore, spin-triplet Josephson junctions have also been proposed for use in quantum computing, specifically in the implementation of qubits and quantum gates [118]. The controllability of the ground-state phase difference between 0 and π in spin-triplet junctions allows the implementation of phase qubits, which are one of the three types of superconducting qubits [119,120]. Phase qubits rely on the manipulation of the phase difference between two superconducting islands, and the use of a spin-triplet junction as the coupling element in such qubits has been shown to offer improved performance compared to using a spin-singlet junction [121].

Outlook and Perspectives

This review is organized around the emergence and most updated progress of the two main types of superconducting spintronics application, namely, spin-related logics and memories, from the aspects of underlying mechanisms, materials, to device structures. Strategic combinations of s-wave superconductors with ferromagnets as hybrid superconducting structures facilitate a new superconducting state that indicates the potential for mediating dissipationless spin current, and the idea of introducing superconductivity into ordinary spintronis is believed to be a promising way to complement both conventional spintronic concepts and device applications, such as the novel physics of spin injection, nonequilibrium spin transport, and infinite magnetoresistance in SC/FM heterostructures. Extensive theoretical and experimental studies have already confirmed such enhancement. Setting aside the technical issues in cryogenic working environments, which is also one of the most elusive problems in constraining the promotion of superconducting spintronic technology, there are indeed typical application scenarios such as high performance cloud computation centers or data centers in which the whole computing/storage systems can be maintained at ultralow temperatures.

Spin-related logic devices, superconducting diodes in particular, are gaining increasing momentum in superconducting spintronics research. The underlying mechanism, SDE, due to its outstanding ability to transport directional charges without energy dissipation at low temperatures makes it a competitive alternative for the construction of ultrahigh-sensitivity detection circuits and modulators with ultralow-power consumption, compared to their conventional semiconductor counterparts [34]. Hence, this concept has consistently nurtured and bolstered the exploration of novel physics, combinations of materials, and engineered architectural designs aimed at enhancing the performance of SDE. Previous research has already recognized numerous promising contenders for observing SDE, ranging from noncentrosymmetric superconductors to structures

based on Josephson junctions and unconventional geometries in the realm of superconductivity, according to the foregoing parts in this review. Apart from the "eureka" moment in boosting research on novel physical mechanisms, nevertheless, further researches on the practicalities of superconducting diodes compatible with modern semiconductor systems in terms of conventional materials, synergy, and integration capabilities with current prevalent fabrication process are still needed for careful consideration. For example, magnetic field-free diodes based on conventional superconductors would be a more convenient and economical approach for designing superconducting diodes [55]. SDEs observed in unconventional structures, especially graphene, topological structures, and carbon nanotubes, indeed offer unique opportunities for application practice and fundamental physics research; the acceptance attitude of the industry might be relatively pessimistic.

Despite great efforts in developing spin-related logic devices, in order to meet the performance requirements, compatible spin-related cryogenic memory technologies are also needed. Specifically in this review, we highlight the potential of both spin-valve and spin-triplet Josephson junctions for utilization in cryogenic memory and quantum computing. While spin-valve junctions are simpler in structure, they require more precise control of the thicknesses of the ferromagnetic layers. Conversely, spin-triplet junctions impose less stringent requirements on the thicknesses of the ferromagnetic layers and hold the promise of higher efficiency and enhanced performance in quantum computing applications. Indeed, the absence of energy dissipation caused by spin-flip processes in spin-triplet junctions is a significant advantage that can lead to higher efficiency and reduced power consumption. Furthermore, the use of spin-triplet superconducting materials can lead to the creation of entirely new device architectures with unique functionalities that are not achievable with traditional superconducting or magnetic devices. For example, spin-triplet Josephson junctions can exhibit long-range triplet superconducting correlations that extend over several micrometers, leading to the possibility of creating spin supercurrents with controllable magnitude and direction. This could be used for creating novel devices such as spin supercurrent switches or spin supercurrent transistors, which could revolutionize the field of spintronics.

In summary, the significance of exploring superconducting spintronic devices is definitely undisputed. The emergence and recent updated progress of these spin-related superconducting devices mentioned in this review attempt to promulgate the inevitable challenges and enlightening opportunities for future practical applications.

Acknowledgments

Funding: This work was supported by the National Key Research and Development Program of China (grant no. 2022YFA1402600), the Natural Science Foundation of China (NSF) (grant no. 52201200), and the Fundamental Research Funds for the Central Universities.

Competing interests: The authors declare that they have no competing interests.

References

1. Finocchio G, di Ventra M, Camsari KY, Everschor-Sitte K, Khalili Amiri P, Zeng Z. The promise of spintronics for unconventional computing. *J Magn Magn Mater*. 2021;521:Article 167506.
2. Liu W, Wong PKJ, Xu Y. Hybrid spintronic materials: Growth, structure and 700 properties. *Prog Mater Sci*. 2019;99:27–105.
3. Guo Z, Yin J, Bai Y, Zhu D, Shi K, Wang G, Cao K, Zhao W. Spintronics for energy- efficient computing: An overview and outlook. *Proc IEEE*. 2021;109(8):1398.
4. Yang G, Ciccarelli C, Robinson JWA. Boosting spintronics with superconductivity. *APL Mater*. 2021;9:Article 050703.
5. Hatami M, Bauer GEW, Zhang Q, Kelly PJ. Thermal spin-transfer torque in magnetoelectronic devices. *Phys Rev Lett*. 2007;99(6):Article 066603.
6. Bauer GEW, Saitoh E, Wees van BJ. Spin caloritronics. *Nat Mater*. 2012;11:391–399.
7. Dieny B, Sousa RC, Hérault J, Papusoi C, Prenat G, Ebels U, Houssameddine D, Rodmacq B, Auffret S, Prejbeanu-Buda L, et al. Chapter two —Spintronic devices for memory and logic applications. *Handb Magn Mater*. 2011;19:107–127.
8. Bernstein K, Cavin RK, Porod W, Seabaugh A, Welser J. Device and architecture outlook for beyond cmos switches. *Proc IEEE*. 2010;98(12):2169–2184.
9. Behin-Aein B, Datta D, Salahuddin S, Datta S. Proposal for an all-spin logic device with built-in memory. *Nat Commun*. 5:266–270.
10. Linder J, Robinson JWA. Superconducting spintronics. *Nat Phys*. 2015;11:307.
11. Tinkham M. *Introduction to superconductivity*. Mineola (NY): Dover Publications; 2004.
12. Buzdin AI. Proximity effects in superconductor-ferromagnet heterostructures. *Rev Mod Phys*. 2005;77(3):935.
13. Bergeret FS, Volkov AF, Efetov KB. Odd triplet superconductivity and related phenomena in superconductor-ferromagnet structures. *Rev Mod Phys*. 2005;77(4):1321.
14. Eschrig M. Spin-polarized supercurrents for spintronics: A review of current progress. *Rep Prog Phys*. 2015;78(10):Article 104501.
15. Oboznov VA, Bolginov VV, Feofanov AK, Ryazanov VV, Buzdin AI. Thickness dependence of the josephson ground states of superconductor-ferromagnet-superconductor junctions. *Phys Rev Lett*. 2006;96(19):Article 197003.
16. Robinson JWA, Piano S, Burnell G, Bell C, Blamire MG. Critical current oscillations in strong ferromagnetic π junctions. *Phys Rev Lett*. 2006;97(17):Article 177003.
17. Eschrig M, Kopu J, Cuevas JC, Schön G. Theory of half-metal/superconductor heterostructures. *Phys Rev Lett*. 2003;90(13):Article 137003.
18. Keizer RS, Goennenwein STB, Klapwijk TM, Miao G, Xiao G, Gupta A. A spin triplet supercurrent through the half-metallic ferromagnet CrO2. *Nature*. 2006;439(7078):825–827.
19. Huang J, Fu R, Ye X, Fan D. A survey on superconducting computing technology: Circuits, architectures and design tools. *CCF Trans High Perform Comput*. 2022;4:1–22.
20. Holmes DS, Ripple AL, Manheimer MA. Energy-efficient superconducting computing—Power budgets and requirements. *IEEE Trans Appl Supercond.* 2013;23(3):1701610.
21. Braginski AI. Superconductor electronics: Status and outlook. *J Supercond Nov Magn*. 2019;32:23–44.
22. Robinson J. A boost for superconducting logic. *Physics*. 2015;8:49.
23. Keyes RW. Physics, and transistors in computers. *Contemp Phys*. 2009;50(6):647.

24. Rikken GLJA, Fölling J, Wyder P. Electrical magnetochiral anisotropy. *Phys Rev Lett*. 2001;87(23):Article 236602.
25. Rikken GLJA, Wyder P. Magnetoelectric anisotropy in diffusive transport. *Phys Rev Lett*. 2005;94(1): Article 016601.
26. Tokura Y, Nagaosa N. Nonreciprocal responses from non-centrosymmetric quantum materials. *Nat Commun*. 2018;9(1):3740.
27. Nadeem M, Fuhrer MS, Wang X. Superconducting diode effect—Fundamental concepts, material aspects, and device prospects. arXiv:2301.13564 (2023).
28. Wakatsuki R, Saito Y, Hoshino S, Itahashi YM, Ideue T, Ezawa M, Iwasa Y, Nagaosa N. Nonreciprocal charge transport in noncentrosymmetric superconductors. *Sci Adv*. 2017;3(4):Article e1602390.
29. Itahashi YM, Ideue T, Saito Y, Shimizu S, Ouchi T, Nojima T, Iwasa Y. Nonreciprocal transport in gate-induced polar superconductor $SrTio_3$. *Sci Adv*. 2020;6(13): Article eaay9120.
30. Zhang E, Xu X, Zou Y-C, Ai L, Dong X, Huang C, Leng P, Liu S, Zhang Y, Jia Z, et al. Nonreciprocal superconducting *nbse*$_2$ antenna. *Nat Commun*. 2020;11(1):5634.
31. Saito Y, Kasahara Y, Ye J, Iwasa Y, Nojima T. Metallic ground state in an ion-gated two-dimensional superconductor. *Science*. 2015;350(6259):409.
32. Baumgartner C, Fuchs L, Costa A, Reinhardt S, Gronin S, Gardner GC, Lindemann T, Manfra MJ, Faria PE Jr, Kochan D, et al. Supercurrent rectification and magnetochiral effects in symmetric josephson junctions. *Nat Nanotechnol*. 2022;17(1):39–44.
33. Edelstein VM. The Ginzburg-Landau equation for superconductors of polar symmetry. *J Phys Condens Matter*. 1996;8(3):339.
34. Ando F, Miyasaka Y, Li T, Ishizuka J, Arakawa T, Shiota Y, Moriyama T, Yanase Y, Ono T. Observation of superconducting diode effect. *Nature*. 2020;584(7821):373–376.
35. Wu H, Wang Y, Xu Y, Sivakumar PK, Pasco C, Filippozzi U, Parkin SSP, Zeng Y-J, McQueen T, Ali MN. The field-free josephson diode in a van der waals heterostructure. *Nature*. 2022;604(7907):653.
36. Ilicć S, Bergeret FS. Theory of the supercurrent diode effect in rashba superconductors with arbitrary disorder. *Phys Rev Lett*. 2022;128(17):Article 177001.
37. Pal B, Chakraborty A, Sivakumar PK, Davydova M, Gopi AK, Pandeya AK, Krieger JA, Zhang Y, Date M, Ju S, et al. Josephson diode effect from cooper pair momentum in a topological semimetal. *Nat Phys*. 2022;18(10):1228.
38. Daido A, Ikeda Y, Yanase Y. Intrinsic superconducting diode effect. *Phys Rev Lett*. 2022;128(3):Article 037001.
39. Yuan NFQ, Fu L. Supercurrent diode effect and finite-momentum superconductors. *Proc Natl Acad Sci*. 2022;119(15):Article e2119548119.
40. He JJ, Tanaka Y, Nagaosa N. A phenomenological theory of superconductor diodes. *New J Phys*. 2022;24:Article 053014.
41. Lyu Y-Y, Jiang J, Wang Y-L, Xiao Z-L, Dong S, Chen Q-H, Milošević MV, Wang H, Divan R, Pearson JE, et al. Superconducting diode effect via conformal-mapped nanoholes. *Phys Rev Lett*. 2016;12:2703.
42. Lin J-X, Siriviboon P, Scammell HD, Liu S, Rhodes D, Watanabe K, Taniguchi T, Hone J, Scheurer MS, JIA L. Zero-field superconducting diode effect in small-twist-angle trilayer graphene. *Nat Phys*. 2022;18:1221.
43. Narita H, Ishizuka J, Kawarazaki R, Kan D, Shiota Y, Moriyama T, Shimakawa Y, Ognev AV, Samardak AS, Yanase Y, et al. *Nat Nanotechnol*. 2022;17(8):823.
44. Bauriedl L, Bäuml C, Fuchs L, Baumgartner C, Paulik N, Bauer JM, Lin K-Q, Lupton JM, Taniguchi T, Watanabe K, et al. Supercurrent diode effect and magnetochiral anisotropy in few-layer $NbSe_2$. *Nat Commun*. 2022;13:4266.
45. Jiang H-M, Pan X-Y. Local breaking of the spin degeneracy in the vortex states of ising superconductors: Induced antiphase ferromagnetic order. *Phys Rev B*. 2022;105(1):Article 014510.
46. Wickramaratne D, Mazin II. Mazin II. Ising superconductivity: A first-principles perspective. arXiv:2304.03759 (2023).
47. Kealhofer R, Jeong H, Rashidi A, Balents L, Stemmer S. Anomalous superconducting diode effect in a polar superconductor. *Phys Rev B*. 2023;107(10):L100504.
48. Sundaresh A, Väyrynen JI, Lyanda-Geller Y, Rokhinson LP. Diamagnetic mechanism of critical current non-reciprocity in multilayered superconductors. *Nat Commun*. 2023;14:Article 1628.
49. Du W-S, Chen W, Zhou Y, Zhou T, Liu G, Zhang Z, Miao Z, Jia H, Liu S, Zhao Y, et al. Superconducting diode effect and large magnetochiral anisotropy in t_d-mote$_2$ thin film. arXiv:2303.09052 (2023).
50. Hou Y, Nichele F, Chi H, Lodesani A, Wu Y, Ritter MF, Haxell DZ, Davydova M, Ilić S, Glezakou-Elbert O. et al, Ubiquitous superconducting diode effect in superconductor thin films. *Phys Rev Lett*. 2023;131(2):Article 027001.
51. Hu J, Wu C, Dai X. Proposed design of a josephson diode. *Phys Rev Lett*. 2007;99(6):Article 067004.
52. Misaki K, Nagaosa N. Theory of the nonreciprocal josephson effect. *Phys Rev B*. 2021;103(24):Article 245302.
53. Baumgartner C, Fuchs L, Costa A, Picó-Cortés J, Reinhardt S, Gronin S, Gardner GC, Lindemann T, Manfra MJ, Faria Junior PE, et al. Effect of rashba and dresselhaus spin-orbit coupling on supercurrent rectification and magnetochiral anisotropy of ballistic josephson junctions. *J Phys: Condens Matter*. 2022;34:Article 154005.
54. Jeon K-R, Kim J-K, Yoon J, Jeon J-C, Han H, Cottet A, Kontos T, Parkin SSP. Zero-field polarity-reversible josephson supercurrent diodes enabled by a proximity-magnetized pt barrier. *Nat Mater*. 2022;21(9):1008–1013.
55. Jiang J, Milošević MV, Wang YL, Xiao ZL, Peeters FM, Chen QH. Field-free superconducting diode in a magnetically nanostructured superconductor. *Phys Rev Appl*. 2022;18(3):Article 034064.
56. Golod T, Krasnov VM. Demonstration of a superconducting diode-with-memory, operational at zero magnetic field with switchable nonreciprocity. *Nat Commun*. 2022;13: Article 3658.
57. Hou Y, Nichele F, Chi H, Lodesani A, Wu Y, Ritter MF, Haxell DZ, Davydova M, Ilić S, Glezakou-Elbert O. et al, Ubiquitous superconducting diode effect in superconductor thin films. *Phys Rev Lett*. 2023;131(2):Article 027001.
58. Díez-Mérida J, Díez-Carlón A, Yang SY, Xie Y-M, Gao X-J, Senior J, Watanabe K, Taniguchi T, Lu X, Higginbotham AP, et al. Symmetry-broken josephson junctions and superconducting diodes in magic-angle twisted bilayer graphene. *Nat Commun*. 2023;14:Article 2396.
59. Pal B, Chakraborty A, Sivakumar PK, Davydova M, Gopi AK, Pandeya AK, Krieger JA, Zhang Y, Date M, Ju S, et al. Josephson diode effect from cooper pair momentum in a topological semimetal. *Nat Phys*. 2022;18(10):1228.

60. Yasuda K, Yasuda H, Liang T, Yoshimi R, Tsukazaki A, Takahashi KS, Nagaosa N, Kawasaki M, Tokura Y. Nonreciprocal charge transport at topological insulator/superconductor interface. *Nat Commun*. 2019;10(1):2734.
61. Masuko M, Kawamura M, Yoshimi R, Hirayama M, Ikeda Y, Watanabe R, He JJ, Maryenko D, Tsukazaki A, Takahashi KS, et al. Nonreciprocal charge transport in topological superconductor candidate bi2te3/PdTe2 heterostructure. *npj Quantum Mater*. 2022;7(1):104.
62. van't Erve OMJ, Friedman AL, Cobas E, Li CH, Robinson JT, Jonker BT. Low-resistance spin injection into silicon using graphene tunnel barriers. *Nat Nanotechnol*. 7(11):737–742.
63. Scammell HD, Li JIA, Scheurer MS. Theory of zero-field superconducting diode effect in twisted trilayer graphene. *2D Mater*. 2022;9(2):Article 025027.
64. Narlikar A. *The Oxford handbook of small superconductors*. Oxford (UK): Oxford University Press; 2017.
65. Gupta M, Graziano GV, Pendharkar M, Dong JT, Dempsey CP, Palmstrøm C, Pribiag VS. Superconducting diode effect in a three-terminal josephson device. arXiv:2206.08471 (2022).
66. de Picoli T, Blood Z, Lyanda-Geller Y, Väyrynen JI. Superconducting diode effect in quasi-one-dimensional systems. *Phys Rev B*. 2023;107(22):Article 224518.
67. Trahms M, Melischek L, Steiner JF, Mahendru B, Tamir I, Bogdanoff N, Peters O, Reecht G, Winkelmann CB, von Oppen F, et al. Diode effect in josephson junctions with a single magnetic atom. *Nature*, 2023;615(7953):628.
68. Scheick L, Guertin S, Swift G. Analysis of radiation effects on individual dram cells. *IEEE Trans Nucl Sci*. 2000;47(6):2534.
69. Yoshikawa N, Tomida T, Tokuda M, Liu Q, Meng X, Whiteley SR, VanDuzer T. Characterization of 4 k cmos devices and circuits for hybrid josephson-cmos systems. *IEEE Trans Appl Supercond*. 2005;15(2):267.
70. Patra B, Incandela RM, van Dijk JPG, Homulle HAR, Song L, Shahmohammadi M, Staszewski RB, Vladimirescu A, Babaie M, Sebastiano F, et al. Cryo-cmos circuits and systems for quantum computing applications. *IEEE J Solid State Circuits*. 2018;53:309.
71. Wang F, Vogelsang T, Haukness B, Magee SC. DRAM retention at cryogenic temperatures. In: *2018 IEEE International Memory Workshop (IMW)*. Kyoto: IEEE; 2018. p. 1–4.
72. Ahn C, Kim S, Gokmen T, Dial O, Ritter M, Wong H-S P. Temperature-dependent studies of the electrical properties and the conduction mechanism of hfox-based rram. Paper presented at: Proceedings of Technical Program - 2014 International Symposium on VLSI Technology, Systems and Application (VLSI-TSA); 2014 Aug 28–30; Hsinchu, Taiwan
73. Hu VP-H, Liu C-J. Static noise margin analysis for cryo-cmos sram cell. Paper presented at: IEEE International Symposium on Radio-Frequency Integration Technology (RFIT); 2021 Aug 25–27; Hualien, Taiwan.
74. Sanuki T, Aiba Y, Tanaka H, Maeda T, Sawa K, Kikushima F, Miura M. Cryogenic operation of 3-d flash memory for storage performance improvement and bit cost scaling. *IEEE J Explor Solid-State Comput Dev Circ*. 2021;7(2):159.
75. Hu VP-H, Su CW, Lee YW, Ho TY, Cheng CC, Chen TC, Hung TYT, Li JF, Chen YG, Li LJ. Energy-efficient monolithic 3-d sram cell with beol mos2 fets for soc scaling. *IEEE Trans Electron Dev*. 2020;67(10):4216–4221.
76. Sun J-C, Taur Y, Dennard R, Klepner S. Submicrometer-channel cmos for low-temperature operation. *IEEE Trans Electron Dev*. 1987;34(1):19–27.
77. Wang P, Peng X, Chakraborty W, Khan A, Datta S, Yu S. Cryogenic performance for compute-in-memory based deep neural network accelerator. Paper presented at: IEEE International Symposium on Circuits and Systems (ISCAS); 2021 May 22–28; Daegu, Korea.
78. Beckers A, Jazaeri F, Enz C. Characterization and modeling of 28-nm bulk cmos technology down to 4.2 k. *IEEE J Electron Devices Soc*. 2018;6:1007–1018.
79. M. Barlow, G. Fu, B. Hollosi, C. Lee, J. Di, H. A. Mantooth, M. Schupbach, R. Berger. A pFET-access radiation-hardened SRAM for extreme environments. Paper presented at: 2008 51st Midwest Symposium on Circuits and Systems; 2008 Aug 10–13; Knoxville, TN, USA.
80. Song YJ, Lee JH, Shin HC, Lee KH, Suh K, Kang JR, Pyo SS, Jung HT, Hwang SH, Koh GH, et al. Highly functional and reliable 8mb STT-MRAM embedded in 28 nm logic. Paper presented at: 2016 IEEE International Electron Devices Meeting (IEDM); 2016 December; San Francisco, CA, USA. p. 27.2.1–27.2.4.
81. Tehrani S, Slaughter JM, Chen E, Durlam M, Shi J, DeHerren M. Progress and outlook for MRAM technology. *IEEE Trans Nucl Sci*. 35(5):2814.
82. Rehm L, Wolf G, Kardasz B, Pinarbasi M, Kent AD. Sub-nanosecond spin-torque switching of perpendicular magnetic tunnel junction nanopillars at cryogenic temperatures. *Appl Phys Lett*. 2019;115(18):Article 182404.
83. Lang L, Jiang Y, Lu F, Wang C, Chen Y, Kent AD, Ye L. A low temperature functioning CoFeB/MgO-based perpendicular magnetic tunnel junction for cryogenic nonvolatile random access memory. *Appl Phys Lett*. 2020;116(2):Article 022409.
84. Garzón E, Rose De R, Crupi F, Carpentieri M, Teman A, Lanuzza M. Simulation analysis of DMTJ-based STT-MRAM operating at cryogenic temperatures. *IEEE Trans Magn*. 2021;57(7):1–6.
85. Tagirov LR. Low-field superconducting spin switch based on a superconductor/ferromagnet multilayer. *Phys Rev Lett*. 1999;83:2058–2061.
86. Moraru IC, Pratt WP, Birge NO. Magnetization-dependent $t - c$ shift in ferromagnet/superconductor/ferromagnet trilayers with a strong ferromagnet. *Phys Rev Lett*. 96:Article 037004.
87. Li B, Roschewsky N, Assaf BA, Eich M, Epstein-Martin M, Heiman D, Münzenberg M, Moodera JS. Superconducting spin switch with infinite magnetoresistance induced by an internal exchange field. *Phys Rev Lett*. 2013;110(9): Article 097001.
88. Tedrow PM, Meservey R, Schwartz BB. Experimental evidence for a first-order magnetic transition in thin superconducting aluminum films. *Phys Rev Lett*. 24(18):1004.
89. Zhu Y, Pal A, Blamire MG, Barber ZH. Superconducting exchange coupling between ferromagnets. *Nat Mater*. 2017;16(2):195.
90. Gu Y, Halász GB, Robinson JWA, Blamire MG. Large superconducting spin valve effect and ultrasmall exchange splitting in epitaxial rare-earth-niobium trilayers. *Phys Rev Lett*. 2015;115(6):Article 067201.
91. Anderson PW, Dayem AH. Radio-frequency effects in superconducting thin film bridges. *Phys Rev Lett*. 1964;13(6):195.

92. Tahara S, Ishida I, Ajisawa Y, Wada Y. Experimental vortex transitional nondestructive read-out josephson memory cell. *J Appl Phys*. 1989;65(2):851.
93. Yuh P-F. A buffered nondestructive-readout josephson memory cell with three gates. *IEEE Trans Magn*. 1991;27(2):2876.
94. Yuh P-F. A 2-kbit superconducting memory chip. *IEEE Trans Appl Supercond*. 1993;3(2):3013–3021.
95. Polonsky S, Kirichenko A, Semenov V, Likharev K. Rapid single flux quantum random access memory. *IEEE Trans Appl Supercond*. 1995;5(2):3000–3005.
96. Alam S, Jahangir MA, Aziz A. A compact model for superconductor- insulator-superconductor (SIS) josephson junctions. *IEEE Electron Device Lett*. 2020;41(8):1249–1252.
97. Ryazanov VV, Bol'ginov VV, Sobanin DS, Vernik IV, Tolpygo SK, Kadin AM, Mukhanov OA. Magnetic josephson junction technology for digital and memory applications. *Phys Proced*. 2015;36:35.
98. Demler EA, Arnold GB, Beasley MR. Superconducting proximity effects in magnetic metals. *Phys Rev B*. 1997;55(22):Article 15174.
99. Larkin TI, Bol'ginov VV, Stolyarov VS, Ryazanov VV, Vernik IV, Tolpygo SK, Mukhanov OA. Ferromagnetic josephson switching device with high characteristic voltage. *Appl Phys Lett*. 2012;100:Article 222601.
100. Niedzielski BM, Diesch SG, Gingrich EC, Wang Y, Loloee R, Pratt WP, Birge NO. Use of pd-fe and ni-fe-nb as soft magnetic layers in ferromagnetic josephson junctions for nonvolatile cryogenic memory. *IEEE Trans Appl Supercond*. 2014;24(4):1–7.
101. Bhatia E, Senapati K. Aspects of long range spin-triplet correlations in superconductor/ferromagnet hetero-structures. *Supercond Sci Technol*. 2022;35(9):Article 094004.
102. Bergeret FS, Volkov AF, Efetov KB. Long-range proximity effects in superconductor-ferromagnet structures. *Phys Rev Lett*. 2001;86(18):4096.
103. Beenakker CWJ. Annihilation of colliding bogoliubov quasiparticles reveals their majorana nature. *Phys Rev Lett*. 2014;112(7):Article 070604.
104. Yamashita T, Takahashi S, Imamura H, Maekawa S. Spin transport and relaxation in superconductors. *Phys Rev B*. 2002;65(17):Article 172509.
105. Yang H, Yang S-H, Takahashi S, Maekawa S, Parkin SSP. Extremely long quasiparticle spin lifetimes in superconducting aluminium using MgO tunnel spin injectors. *Nat Mater*. 2010;9(7):586.
106. Quay CHL, Chevallier D, Bena C, Aprili M. Spin imbalance and spin-charge separation in a mesoscopic superconductor. *Nat Phys*. 2013;9:84.
107. Gu JY, Caballero JA, Slater RD, Loloee R, Pratt WP. Direct measurement of quasiparticle evanescent waves in a dirty superconductor. *Phys Rev B*. 2002;66(14):Article 140507.
108. Khaire TS, Khasawneh MA, Pratt WP, Birge NO. Observation of spin-triplet superconductivity in co-based josephson junctions. *Phys Rev Lett*. 2010;104(13):Article 137002.
109. Oh S, Youm D, Beasley MR. A superconductive magnetoresistive memory element using controlled exchange interaction. *Appl Phys Lett*. 1997;71(16):2376.
110. Fominov YV, Golubov AA, Karminskaya TY, Kupriyanov MY, Deminov RG, Tagirov LR. Superconducting triplet spin valve. arXiv:1002.2113 (2010).
111. Miao G-X, Ramos AV, Moodera JS. Infinite magnetoresistance from the spin dependent proximity effect in symmetry driven bcc-fe/v/fe heteroepitaxial superconducting spin valves. *Phys Rev Lett*. 2008;101(13):Article 137001.
112. Lenk D, Morari R, Zdravkov VI, Ullrich A, Khaydukov Y, Obermeier G, Müller C, Sidorenko AS, Krug von Nidda H-A, et al. Full-switching FSF-type superconducting spin-triplet magnetic random access memory element. *Phys Rev B*. 2017;96(18):Article 184521.
113. Birge NO, Houzet M. Spin-singlet and spin-triplet josephson junctions for cryogenic memory. *IEEE Magn Lett*. 10:1–5.
114. Martinez WM, Pratt WP, Birge NO. Amplitude control of the spin-triplet supercurrent in **s/f/s** josephson junctions. *Phys Rev Lett*. 2016;116(7):Article 077001.
115. Glick JA, Aguilar V, Gougam AB, Niedzielski BM, Gingrich EC, Loloee R, Pratt WP Jr, Birge NO. Phase control in a spin-triplet SQUID. *Sci Adv*. 2018;4(7):Article eaat9457.
116. Dayton IM, Sage T, Gingrich EC, Loving MG, Ambrose TF, Siwak NP, Keebaugh S, Kirby C, Miller DL, et al. Experimental demonstration of a Josephson magnetic memory cell with a programmable π-junction. *IEEE Magn Lett*. 2018;9(1):Article 3301905.
117. Gingrich EC, Niedzielski BM, Glick JA, Wang Y, Miller DL, Loloee R, Pratt WP Jr, Birge NO. Controllable 0-π josephson junctions containing a ferromagnetic spin valve. *Nat Phys*. 2016;12:564–567.
118. Wei H-R, Deng F-G. Universal quantum gates on electron-spin qubits with quantum dots inside single-side optical microcavities. *Opt Express*. 2014;22(1):593–607.
119. Caruso R, Massarotti D, Campagnano G, Pal A, Ahmad HG, Lucignano P, Eschrig M, Blamire MG, Tafuri F. Tuning of magnetic activity in spin-filter josephson junctions towards spin-triplet transport. *Phys Rev Lett*. 122(4):Article 047002.
120. Guo G-L, Leng H-B, Hu Y, Liu X. 0-π qubit with one josephson junction. *Phys Rev B*. 2022;105:Article L180502.
121. Wei LF, Johansson JR, Cen LX, Ashhab S, Nori F. Controllable coherent population transfers in superconducting qubits for quantum computing. *Phys Rev Lett*. 2008;100(21):Article 113601.
122. Jiang K, Hu J. Superconducting diode effects. *Nat Phys*. 2022;18:1145–1146.
123. Ohnishi K, Komori S, Yang G, Jeon K-R, Olde Olthof LAB, Montiel X, Blamire MG, Robinson JWA. Spin-transport in superconductors. *Appl Phys Lett*. 116(13):Article 130501.

Advanced Devices & Instrumentation
A SCIENCE PARTNER JOURNAL

Spin-Related Superconducting Devices for Logic and Memory Applications

Yu He, Jiaxu Li, Qiusha Wang, Hisakazu Matsuki, and Guang Yang

Citation: He Y, Li J, Wang Q, Matsuki H, Yang G. Spin-Related Superconducting Devices for Logic and Memory Applications. *Adv Devices Instrum*. 2023;**4**:0035. DOI: 10.34133/adi.0035

Recently, there has been a surge of research in the field of superconducting spintronics, which combines superconductivity and magnetism. This emerging field is considered an alternative or complementary approach to traditional complementary metal-oxide semiconductor (CMOS) technology, offering high efficiency and effectiveness. Furthermore, the unique physical phenomena resulting from the interplay of these two competing properties have attracted increasing attention for their potential application in low-power quantum computing. In this review, we focus on the latest advancements in spin-related superconducting logic devices, specifically categorized as superconducting diodes based on their semiconductor counterparts. Additionally, given the ultralow operating temperatures required for these devices, we provide a comprehensive overview of compatible cryogenic memory technologies that incorporate spin-related principles. Finally, we address the key challenges currently hindering the practical implementation of spin-related superconducting electronics and offer insights and directions for future research in this field.
Image

Advanced Devices & Instrumentation (ISSN 2767-9713) is published by the American Association for the Advancement of Science. 1200 New York Avenue NW, Washington, DC 20005.